ADVANCED INTELLIGENT SYSTEMS
Open Access
www.advintellsyst.com

Magnetic Actuation Systems for Miniature Robots: A Review

*Zhengxin Yang and Li Zhang**

A magnetic field, which is transparent and relatively safe to biological tissue, is a powerful tool for remote actuation and wireless control of magnetic devices. Furthermore, miniature robots can access complex and narrow regions of the human body as well as manipulate down to subcellular entities; however, integrating onboard components is difficult due to their limited size. Combining these two technologies, magnetic miniature robots have undergone rapid development during the past two decades, mainly because of their high potential in medical and bioengineering applications. To improve the scientific and clinical outcomes of these tiny agents, developing suitable and reliable actuation systems is essential. As a newly emerging field that has progressed in recent years, magnetic actuation systems offer a harmless and effective approach for the remote control of miniature robots via a dynamic magnetic field. Herein, a review on the state-of-the-art magnetic actuation systems for miniature robots is presented with the goal of providing readers with a better understanding of magnetic actuation and guidance for future system design.

1. Introduction

Miniature robots have attracted increasing attention in recent years, mainly because of their high potential in medical and bioengineering applications.[1–6] The term "miniature robot" refers to a controllable device with a size ranging from micrometers to millimeters.[7] Because of their small scale, these robots can access complex and narrow regions of the human body in a minimally invasive manner, for example, in the gastrointestinal (GI) tract, vasculature, brain, and eye.[8] Moreover, they have the potential to perform various tasks, such as targeted delivery,[9,10] precise surgery,[11,12] and medical examination.[13,14] In addition, microsized robots have prospects for in vitro applications, such as cell manipulation and tissue engineering, because of their capability to manipulate down to subcellular entities with high precision and repeatability.[15,16]

Owing to their small size, the developed tiny agents are expected to reshape the medical diagnosis and treatment with minimally invasive procedures. However, integrating conventional onboard components (e.g., actuators, processors, and power sources) becomes very difficult due to the restricted volume, especially for submillimeter robots. To date, diverse strategies have been proposed, such as chemical, optical, ultrasonic, electrostatic, and magnetic actuation.[17,18] Among these, magnetic actuation is one of the preferred strategies because it is transparent and relatively safe to biological tissues and it has good controllability.[19,20] Even for robots in millimeter scales, motivated by the simultaneous pursuit of good maneuverability and minimal invasion, the contradiction between active modality and small size always exists for the onboard design, and using offboard magnetic actuation has become a feasible solution.[21–23] Therefore, magnetic miniature robots have been widely developed.[24]

The earliest example of magnetic manipulation applied in the medical field can probably date back to ancient India, when the lodestone was used to attract foreign bodies beneath the skin.[25] The first demonstration applying the magnetic method in biology may have started in Germany in the early 1920s, when the viscosity of the protoplast was observed under electromagnetic fields.[26] To improve the scientific and clinical outcomes of magnetic miniature robots, developing proper and reliable actuation systems that generate required magnetic fields is necessary. Both permanent magnets and electromagnets are good candidates for the generation of magnetic field. Integrated with accessories (e.g., servo motors and current amplifiers), a variety of magnetic actuation systems have been developed.[27–31] These systems are versatile in terms of magnetic actuation. Some can generate multidirectional uniform magnetic fields and conduct 2 or 3-degrees of freedom (DOF) pure torque control,[32,33] some are able to produce arbitrary magnetic field gradients and manage 2 or 3-DOF pure force propulsion,[34,35] and some are capable of directing

Z. Yang, Prof. L. Zhang
Department of Mechanical and Automation Engineering
The Chinese University of Hong Kong
Shatin NT, Hong Kong, China
E-mail: lizhang@cuhk.edu.hk

Prof. L. Zhang
CUHK T Stone Robotics Institute
The Chinese University of Hong Kong
Shatin NT, Hong Kong, China

Prof. L. Zhang
Chow Yuk Ho Technology Centre for Innovative Medicine
The Chinese University of Hong Kong
Shatin NT, Hong Kong, China

The ORCID identification number(s) for the author(s) of this article can be found under https://doi.org/10.1002/aisy.202000082.

DOI: 10.1002/aisy.202000082

up to 6-DOF actuation by combining both force and torque control.[28,36] The ability to generate a magnetic field is determined by the configuration and algorithm of the system, whereas the requisite magnetic field is dominated by the controlled robot, which is also viewed as the remote end effector of the system. Some actuation systems aim to create a specific type of field, and others contain multiple modes to accommodate different end effectors. Moreover, the workspace of the existing magnetic actuation systems covers from a few millimeters to tens of centimeters, which basically depends on the working scenario (e.g., in vitro micromanipulation[37] and in vivo medical treatment[38]) and relates to the system configuration. Another reason is that developing magnetic actuation systems for miniature robots is a newly emerging field that has just expanded in the last decade; therefore, many planned human-scale facilities have only been built as proof-of-concept prototypes at the current stage.

The system review mainly focuses on the configurations of the current magnetic actuation systems and their capability of magnetic field generation, de-emphasizing the controlled device and the specific workspace for the preceding reasons, which are discussed intensively in the subsequent sections. This review article intends to provide an overview of the state-of-the-art magnetic actuation systems for miniature robots, as well as a better understanding of magnetic actuation and a reference for future system design. The principles of magnetic actuation and sources of field generation are briefly described at the beginning. Then, permanent magnetic and electromagnetic actuation systems are introduced by category. Subsequently, some typical miniature end effectors and their biomedical applications are presented. Finally, the conclusions and outlooks are discussed.

Zhengxin Yang received her B.E. degree in mechanical design, fabrication, and automation from the Dalian University of Technology, Dalian, China, in 2016, and M.E. degree in mechatronics engineering from the Harbin Institute of Technology, Harbin, China, in 2018. She is currently pursuing a Ph.D. degree in the Department of Mechanical and Automation Engineering, The Chinese University of Hong Kong. Her current research interests include the development of electromagnetic actuation systems and the control of magnetic microrobots and medical robots.

Li Zhang received his Ph.D. degree from the University of Basel, Switzerland, in 2007. From 2007 to 2012, he was with the Institute of Robotics and Intelligent Systems (IRIS), Swiss Federal Institute of Technology (ETH) Zürich, Switzerland, as a postdoctoral fellow and then as a senior scientist. He is currently an associate professor with the Department of Mechanical and Automation Engineering, The Chinese University of Hong Kong. His main research interests include micro/nanorobotics for biomedical applications. He is a distinguished lecturer appointed by IEEE NTC.

2. Magnetic Actuation and Magnetic Fields

First, the governing principles of magnetic actuation are discussed. In addition, the common field generating sources are briefly introduced, including permanent magnets and electromagnets.

2.1. Magnetic Actuation Principle

Magnetic actuation is conducted by imparting force and/or torque on magnetic objects embedded with magnets or made of magnetizable materials through remotely applied magnetic fields (**Figure 1**). Because no current exists in the manipulation area, the quasistatic magnetic field can be described by Maxwell's equation as[39]

$$\begin{aligned} \nabla \cdot \mathbf{B} &= 0 \\ \nabla \times \mathbf{B} &= 0 \end{aligned} \tag{1}$$

where $\mathbf{B}$ is the external magnetic field and ∇ is the gradient operator. The equation implies that the gradient matrix of $\mathbf{B}$ is symmetric and trace free. A magnetic torque $\boldsymbol{\tau}$ acts on a magnetic object $\mathbf{m}$ when misalignment occurs between the magnetization of the object and the orientation of the magnetic field as follows

$$\boldsymbol{\tau} = \mathbf{m} \times \mathbf{B} = \begin{bmatrix} 0 & B_z & -B_y \\ -B_z & 0 & B_x \\ B_y & -B_x & 0 \end{bmatrix} \begin{bmatrix} m_x \\ m_y \\ m_z \end{bmatrix} \tag{2}$$

Moreover, a magnetic force $\mathbf{f}$ exists, when a magnetic object is in a nonuniform magnetic field as follows

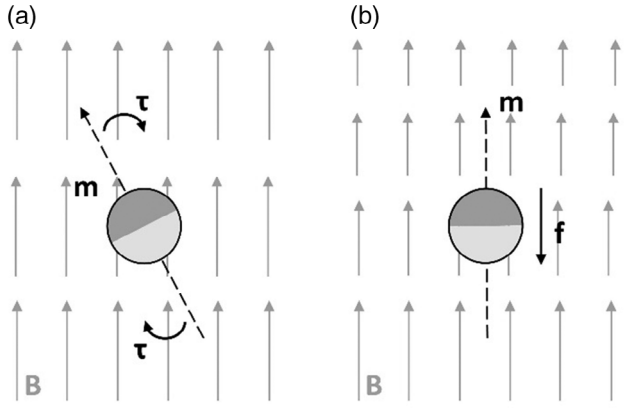

Figure 1. Diagram of magnetic interaction: a) pure torque under a uniform magnetic field; b) pure force under a nonuniform magnetic field.

$$\mathbf{f} = (\mathbf{m}\cdot\nabla)\mathbf{B} = \begin{bmatrix} \frac{\partial B_x}{\partial x} & \frac{\partial B_x}{\partial y} & \frac{\partial B_x}{\partial z} \\ \frac{\partial B_x}{\partial y} & \frac{\partial B_y}{\partial y} & \frac{\partial B_y}{\partial z} \\ \frac{\partial B_x}{\partial z} & \frac{\partial B_y}{\partial z} & -\left(\frac{\partial B_x}{\partial x}+\frac{\partial B_y}{\partial y}\right) \end{bmatrix} \begin{bmatrix} m_x \\ m_y \\ m_z \end{bmatrix} \tag{3}$$

These two effects can execute actuation separately or simultaneously, meaning up to 6-DOF motion control can be conducted. Note that the governing equations (Equation (2) and (3)) abstract the magnetic miniature robots into a dipole, which is reasonable due to the sufficient distances relative to their sizes.[40] Supposing that the magnetic field is fully flexible, only maximal 5-DOF actuation is possible under this dipole approximation (3-DOF force control and 2-DOF torque control) because the robot cannot rotate along its magnetization axis.[28] Indeed, the remaining DOF can be introduced via a force couple using special multimagnet robots; with this, 6-DOF steering is possible.[36,41] Regarding the magnetic field itself, 8-DOF exist (3-DOF magnetic field components and 5-DOF field gradient components).

2.2. Magnetic Field Generation

2.2.1. Permanent Magnets

Permanent magnets have the ability to generate strong and persistent magnetic fields. The strength and distribution of the magnetic field depend on the size and shape of the magnet. The dipole model is widely used because it provides an analytical expression that is convenient for calculation. The magnetic field $\mathbf{B}^{\text{dip}}$ produced by a dipole at a region of interest (ROI) is equal to

$$\mathbf{B}^{\text{dip}} = \frac{\mu_0}{4\pi\|\mathbf{r}\|^3}\left(\frac{3\mathbf{r}\mathbf{r}^T}{\|\mathbf{r}\|^2}-\mathbf{I}\right)\mathbf{M} \tag{4}$$

where μ_0 is the air permeability, $\mathbf{r}$ is the vector pointing from the magnet center to the controlled device, $\mathbf{I}$ is an identity matrix, and $\mathbf{M}$ is the magnetic moment of the dipole source. Because the magnetic field is nonuniform and decreases with the distance, the exerted force $\mathbf{F}^{\text{dip}}$ on a magnetic object $\mathbf{m}$ can be calculated by

$$\mathbf{F}^{\text{dip}} = \frac{3\mu_0}{4\pi\|\mathbf{r}\|^4}\left[\frac{\mathbf{M}\mathbf{r}^T}{\|\mathbf{r}\|}+\frac{\mathbf{r}\mathbf{M}^T}{\|\mathbf{r}\|}-\left(\frac{5\mathbf{r}\mathbf{r}^T}{\|\mathbf{r}\|^2}-\mathbf{I}\right)\frac{\mathbf{M}^T\mathbf{r}}{\|\mathbf{r}\|}\right]\mathbf{m} \tag{5}$$

The aforementioned two expressions are deduced for the magnetic field created by a spherical magnet, and their accuracies increase upon the operating distance. The dipole approximation is also appropriate for nonspherical magnets when the operating distance exceeds two side lengths.[42] This approximation may lose efficacy when the miniature robot is actuated at a short range, in which case other field computation methods need to be considered, such as finite element analysis (FEA)[43] and multipole expansions.[44]

Even for situations not satisfying the dipole approximation, Equation (4) still brings out the fact that two parameters ($\mathbf{r}$ and $\mathbf{M}$, with constant $||\mathrm{M}||$) influence the magnetic field at the ROI; hence, the requisite magnetic field can be obtained by adjusting the position and/or orientation of the permanent magnet. Therefore, permanent magnets are commonly connected with translational and/or rotational mechanisms. As the effects of translation and rotation on the magnetic field and field gradient are nonlinear, control of these systems is often achieved through nonlinear solution methods.[45,46] Equation (5) reveals the faster decrease in field gradient with distance than that of field intensity.

For systems with multiple permanent magnets, the total magnetic field obeys the superposition law. These systems are derived from diverse considerations, such as increasing the uniformity of the magnetic field intensity,[47] programming the specific magnetic field,[48] and simplifying the driven mechanism.[46]

2.2.2. Electromagnets

Electromagnets are capable of producing current-dependent magnetic fields when powered up. There are some specialized coil pairs that generate peculiar magnetic fields. One of the most commonly used is the Helmholtz coil, which is named in honor of the German physician and physicist Hermann von Helmholtz. A Helmholtz coil is composed of two coaxial circular coils with the same radii r, and the interspacing between the coils is equal to r. A nearly uniform magnetic field parallel to the coaxis is produced at the center when equivalent currents flow in the same directions. The Maxwell coil, which is named after the Scottish physicist James Clerk Maxwell, is another specialized coil pair generating an almost uniform field gradient parallel to the coaxis at the center. A Maxwell coil also contains two identical coaxial circular coils with radii r, but the interspacing is $\sqrt{3}r$ and the equant currents are in opposite directions. It is possible to modify both Helmholtz coils and Maxwell coils into square shapes.[49] A saddle coil comprises two identical coils in saddle shape, which coincide with the side surface of a cylinder and symmetric about the coaxis. By parameter optimization, a saddle coil can produce an approximately uniform magnetic field perpendicular to the coaxis when charged with homodromous currents (judged by the straight edge), called the uniform saddle coil.[50] Similarly, a saddle coil can be optimized to generate a nearly uniform field gradient perpendicular to the coaxis when charged with heterodromous currents, referred to as the gradient saddle coil.[51] The Golay coil contains two abreast saddle coils, and the currents in the same saddle coil are homodromous while in different saddle coils are heterodromous, which produces transverse field gradient.[52,53]

For general electromagnets, iron cores made of soft magnetic materials with low hysteresis and high permeability are often installed inside coils to increase the intensity of the magnetic field, which further adds to the complexity of the field distribution. Consequently, using direct dipole approximation to describe their unit-current magnetic field map becomes very difficult. Other strategies, such as the fitted dipole model of the ROI,[28] FEA,[54] and Biot–Savart law-based mathematical model,[55] have been developed by researchers.

The generated magnetic field of an electromagnet depends on the current, and more specifically, the magnetic field generated by the electromagnet without a core and with an unsaturated soft-magnetic core is proportional to the electric current.

In addition, the global magnetic field obeys the superposition law; thus, the components of the magnetic field $\mathbf{B}^{\text{ele}}$ generated by n electromagnets can be derived as

$$\begin{bmatrix} B_x^{\text{ele}} \\ B_y^{\text{ele}} \\ B_z^{\text{ele}} \\ \frac{\partial B_x^{\text{ele}}}{\partial x} \\ \frac{\partial B_x^{\text{ele}}}{\partial y} \\ \frac{\partial B_x^{\text{ele}}}{\partial z} \\ \frac{\partial B_y^{\text{ele}}}{\partial y} \\ \frac{\partial B_y^{\text{ele}}}{\partial z} \end{bmatrix} = \begin{bmatrix} B_{1x}^{\text{ele}} & B_{2x}^{\text{ele}} & \cdots & B_{nx}^{\text{ele}} \\ B_{1y}^{\text{ele}} & B_{2y}^{\text{ele}} & \cdots & B_{ny}^{\text{ele}} \\ B_{1z}^{\text{ele}} & B_{2z}^{\text{ele}} & \cdots & B_{nz}^{\text{ele}} \\ \frac{\partial B_{1x}^{\text{ele}}}{\partial x} & \frac{\partial B_{2x}^{\text{ele}}}{\partial x} & \cdots & \frac{\partial B_{nx}^{\text{ele}}}{\partial x} \\ \frac{\partial B_{1x}^{\text{ele}}}{\partial y} & \frac{\partial B_{2x}^{\text{ele}}}{\partial y} & \cdots & \frac{\partial B_{nx}^{\text{ele}}}{\partial y} \\ \frac{\partial B_{1x}^{\text{ele}}}{\partial z} & \frac{\partial B_{2x}^{\text{ele}}}{\partial z} & \cdots & \frac{\partial B_{nx}^{\text{ele}}}{\partial z} \\ \frac{\partial B_{1y}^{\text{ele}}}{\partial y} & \frac{\partial B_{2y}^{\text{ele}}}{\partial y} & \cdots & \frac{\partial B_{ny}^{\text{ele}}}{\partial y} \\ \frac{\partial B_{1y}^{\text{ele}}}{\partial z} & \frac{\partial B_{2y}^{\text{ele}}}{\partial z} & \cdots & \frac{\partial B_{ny}^{\text{ele}}}{\partial z} \end{bmatrix} \begin{bmatrix} i_1 \\ i_2 \\ \vdots \\ i_n \end{bmatrix} \tag{6}$$

where i_k is the current in the kth electromagnet. Therefore, the total magnetic field at the ROI can be produced by assigning the current of each independent electromagnet in a well-arranged electromagnetic array. Note that for specialized coil pairs, the aforementioned relationship still works, but their special magnetic fields are utilized directly for computation in most cases. Thus, flowing currents are often directly calculable by solving equations derived from Equation (6) on the basis of required magnetic components and coil numbers; optimization algorithms are adopted for multisolution problems.[28,56,57] Movable mechanisms are also integrated into some electromagnetic systems for multiple purposes, such as reducing power dissipation[54] and improving the magnetic field property.[58]

2.3. Magnetic Field Safety

For static and extremely slow time-varying magnetic fields (0–1 Hz), the influence of human beings and living organisms includes magnetohydrodynamic, magnetomechanical, and electronic interactions; thus, restrictions are expressed in terms of the magnetic flux density. It is reported that no consistent biological effect exerts on humans when exposed to magnetic fields below 2 T. The literature indicates no serious adverse health effects from the exposure of healthy people up to 8 T. However, the safety value reduces to 25 mT for people with conductive implants, and 0.5 mT for workers with cardiac pacemakers and electrically active implants.[59]

Dynamic magnetic fields (1 Hz–100 kHz) exert a force on charged particles and result in electric fields and currents in tissues according to Faraday's law; therefore, limitations for such magnetic fields are evaluated by the induced electric field density, the ceiling value of which is frequency-dependent and region-related.[60] The induced electric field is proportional to the magnetic field variation rate and a constant that depends on field distribution, body geometry, and tissue characteristics. A recommended restriction of magnetic field variation rate is expressed as

$$\left|\frac{d\mathbf{B}}{dt}\right| = 20\left(1 + \frac{0.36}{\tau}\right) \tag{7}$$

where τ is the stimulus duration (in ms).[8] This equation is given based on an extensive investigation of peripheral nerve stimulation, which provides a reference to judge the safety of the dynamic magnetic field. The common magnetic fields for actuation purposes are much less than the limitations.

3. Magnetic Actuation Systems

Various actuation systems have been designed for accurate control of magnetic miniature robots. For a clear illustration, the overview of such systems is divided into four categories according to their magnetic sources and configurational characteristics. The controlled magnetic miniature robots, which can be viewed as the remote end effectors of the actuation systems, are abbreviated as devices for simplicity.

3.1. Systems with Permanent Magnets

3.1.1. Single Magnet

A single external permanent magnet can control the translational and rotational motions of the magnetic device by applying a dynamic force and/or torque via changing its pose, which is inexpensive and has high compactness. The early remote actuation utilizing a single magnet is conducted by hand holding magnetic field generators.[21] In these systems, the movement of the permanent magnet greatly depends on the intuition and experience of the operator; therefore, the control performance has high uncertainties. In addition, possible long operating times and imaging radiation are physical challenges for the operator. To overcome these drawbacks, Ciuti et al. connected a permanent cylindrical magnet with a 6-DOF industrial robotic arm, giving a demonstration of using a robot platform to remotely actuate a magnetic device (**Figure 2**a).[61,62] In their scheme, the locomotion of the magnetic device is controlled by the drag force, and the orientation of the magnetic device is steered by the torque moment. To obtain an efficient interaction between the permanent magnet and the controlled device, a virtual magnetic link is designed. The robotic operation is verified to be more precise and reliable than the manual operation. Similar systems adopting commercial robotic manipulators were proposed by other groups, one of which is shown in Figure 2b.[63–65] Strictly speaking, the aforementioned systems have achieved 4-DOF control at most (2-DOF locomotion and 2-DOF orientation) because the magnetic device always contacts with constrained surfaces. Mahoney et al. proposed a system with a similar configuration but a novel control strategy. It takes the total force (e.g., gravity, buoyancy, and the magnetic force) into consideration and well addresses kinematic singularity, realizing 5-DOF control of the device in the open fluid environment.[45]

The direct assembly of a magnet and a commercial robotic manipulator achieves flexible actuation of the device, and the propelling power results from the magnetic field gradient. Another propulsion strategy is via a magnetic torque. A rotational mechanism is introduced as the actuator of a commercial manipulator to provide an extra DOF, through which the permanent magnet can rotate along its own axis with high frequency when driven by the robotic arm, and a rotating magnetic field

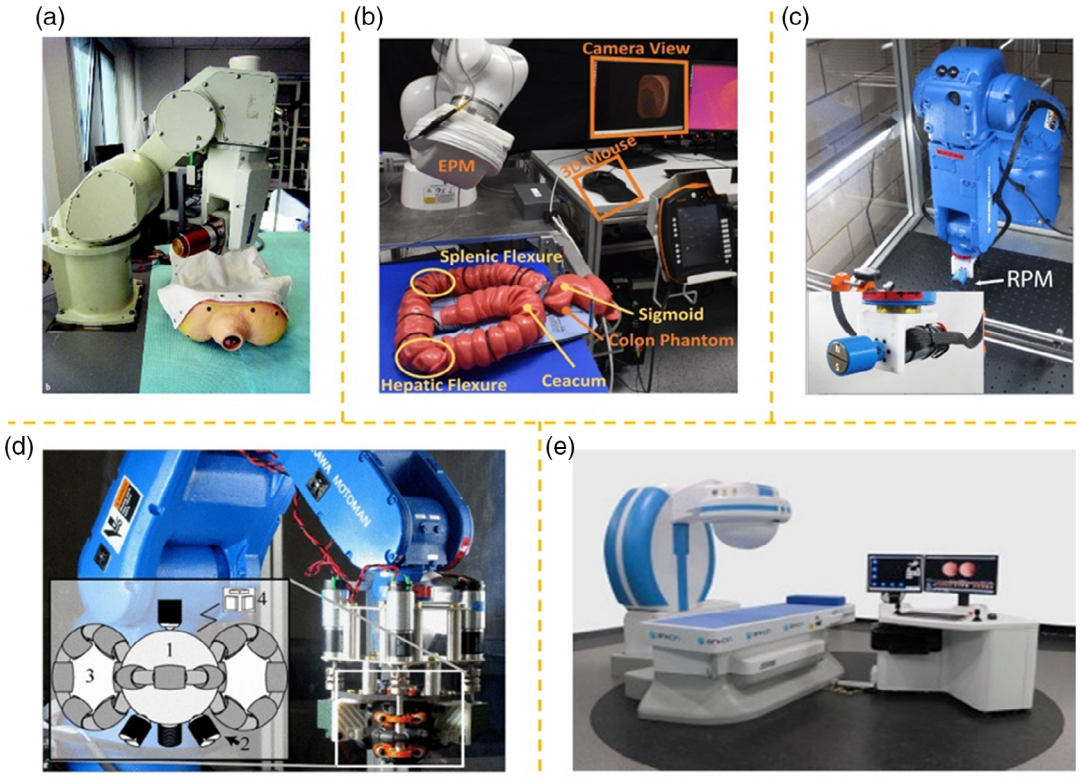

Figure 2. Magnetic actuation systems with a single permanent magnet: a) system using an RV-3SB robotic arm (produced by Mitsubishi Electric); b) system with an LBR Med robotic arm (manufactured by KUKA Robotics Corporation); c) system containing an MH5 robotic arm (produced by Yaskawa Motoman) and a single-axis rotary actuator; d) system consisting of an MH5 robotic arm and a spherical actuator; e) system developed by Ankon Technologies. Panel (a): Reproduced with permission.[62] Copyright 2010, Georg Thieme Verlag KG. Panel (b): Reproduced with permission.[65] Copyright 2019, IEEE. Panel (c): Adapted with permission.[29] Copyright 2014, IEEE. Panel (d): Reproduced with permission.[66] Copyright 2017, IEEE. Panel (e): Reproduced with permission.[67] Copyright 2016, Elsevier.

at the ROI is generated.[68–71] For example, Lee et al. connected a motor-rotating permanent magnet with a 5-DOF SCARA robot, which successfully synchronizes the movement of the permanent magnet with the controlled device.[71] For simplification of the control, the magnetic device is mostly operated in the radial or axial location relative to the magnet, but the unique solution strictly constrains the displacement of the manipulator. To increase the control authority and obstacle avoidance ability of the robotic arm, Mahoney et al. showed the ability to generate an arbitrary rotating magnetic field at the ROI without the preassigned relative position between the permanent magnet and the device (Figure 2c).[29] Therefore, the permanent magnet is capable of planning its own trajectory during actuation instead of just following the controlled device. Figure 2d shows a spherical actuator that contains three omnidirectional wheels and enables the magnet to rotate continuously about any axis.[66] This innovative actuator avoids the kinematic singularities during actuation and enables using robotic manipulators with less DOF.

A commercial actuation system with a single permanent magnet was proposed by Ankon Technologies (Wuhan, China).[67] It is currently powering the capsule endoscopy and has been patented, clinically approved, and installed in many hospitals. The driven mechanism consists of 2 rotational DOF and 3 translational DOF (Figure 2e). The customized robotic mechanism has a reasonable structure and suitable workspace for clinical examination.

3.1.2. Multiple Magnets

Multiple magnets are introduced for various purposes, one of which is to produce a magnetic field with high uniformity for torque actuation because the field gradient can be partly impaired using symmetric distribution. The most representative one is the Niobe system developed by Stereotaxis (Missouri, USA) in 2003, which is currently used for guiding magnetic catheters to treat cardiovascular diseases. The Niobe system has treated over 100 000 patients at more than 100 hospitals globally. In this system, two magnets are distributed on the opposing sides of the bed, each of which can be rotated in a tiltable housing (**Figure 3**a).[72,73] As the gradient generated by each magnet is almost counteracted, this system achieves precise orientation control. Recently, Stereotaxis introduced the Genesis system, which is an upgraded version of the Niobe system, featuring a smaller size, lighter weight, and more flexible movement. Figure 3b shows a system composed of two linear motion stages and two rotatory permanent magnets.[47] During actuation, the magnets follow the controlled device on both sides and rotate

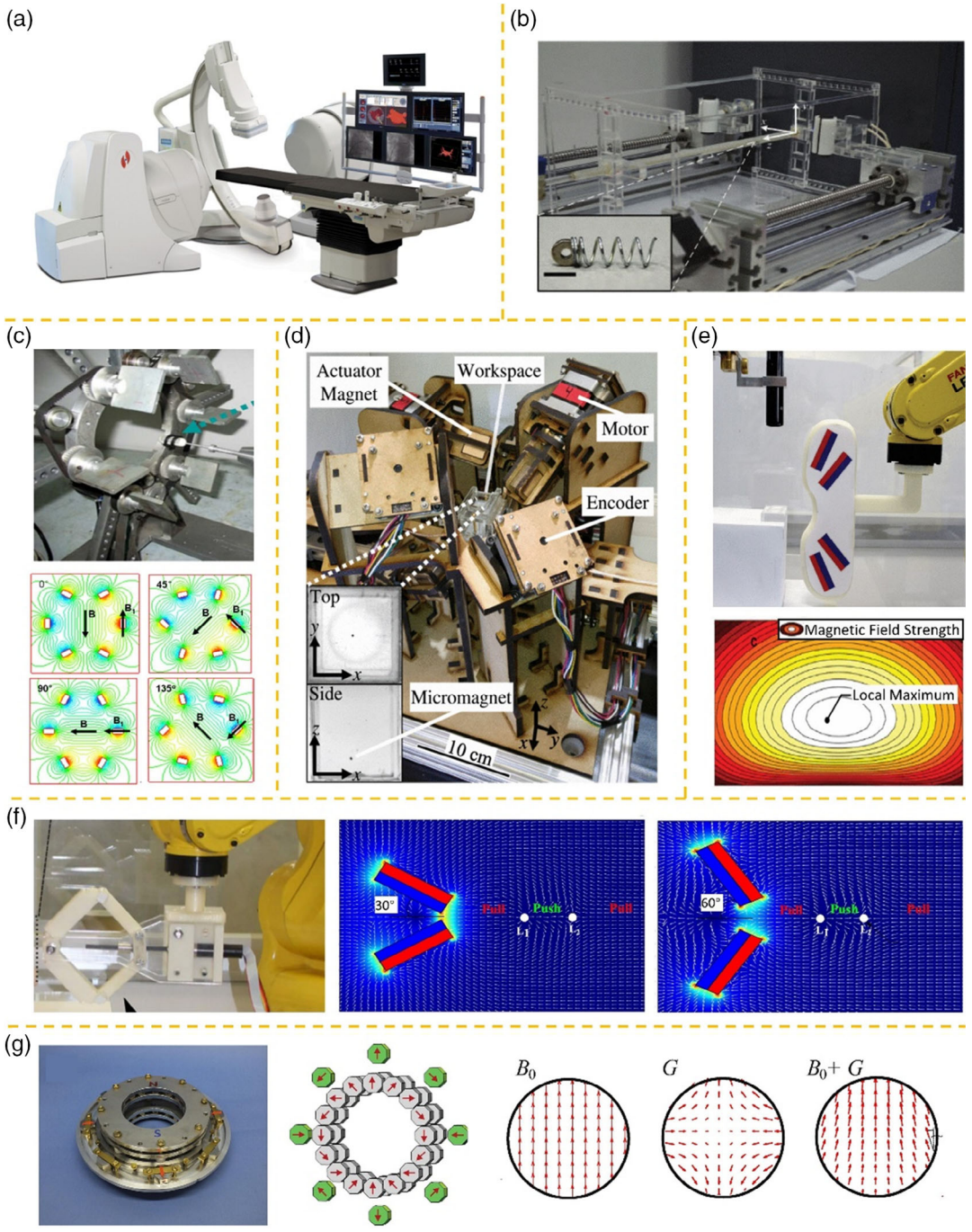

Figure 3. Magnetic actuation systems with multiple permanent magnets: a) Niobe system; b) system with two rotatory permanent magnets; c) system involving six synchronous rotatory magnets; d) system comprising eight independent rotational magnets; e) system consisting of an actuator with four fixed permanent magnets on an LR Mate 200*i*D/4S robotic arm (produced by FANUC Corporation); f) system using an actuator with two movable permanent magnets on an LR Mate 200*i*D/4S robotic arm; g) system with three coaxial Halbach cylinders. Panel (a): Reproduced with permission.[72] Copyright 2007, Wiley Periodicals. Panel (b): Reproduced with permission.[47] Copyright 2014, IEEE. Panel (c): Reproduced with permission.[74] Copyright 2008, IEEE. Panel (d): Adapted with permission.[46] Copyright 2017, IEEE. Panel (e): Adapted with permission.[31] Copyright 2019, IEEE. Panel (f): Adapted with permission.[48] Copyright 2018, Elsevier. Panel (g): Reproduced with permission.[75] Copyright 2017, Elsevier.

synchronously. It has been demonstrated that the rotating magnetic field created by this design has higher uniformity compared with using a single magnet; thus, the controlled device possesses better motion stability. Zhang et al. presented a magnetic actuation system containing six circumferential permanent magnets (Figure 3c).[74] In this system, all magnets are mounted

with allocated initial angles and can rotate along themselves through a synchronous belt-driven mechanism, generating a rotating magnetic field in the center with constant strength and reverse direction. These two systems are incomplete and only realize a 1-DOF propulsion currently, but they are enough for effectiveness verification.

Simplification of the driven mechanism is achieved by using an array of permanent magnets. Ryan et al. proposed a novel actuation system, which adopts eight independent rotatory permanent magnets. Such a system is able to create an omnidirectional magnetic field and field gradient with variable magnitudes (Figure 3d).[46] Although not all 8-DOF magnetic components are decoupled, this system guarantees both torque and force actuation. Meanwhile, it requires no perilous translational motion of the magnets, and offers a new idea of devising magnetic actuation systems.

Specific magnetic fields can be programmed utilizing well-arranged magnets. Zarrouk et al. presented an actuation system that is applicable to open-loop control (Figure 3e).[31] More specifically, a novel actuator with four strip-shaped magnets and a fixture is devised, which is mounted on a commercial robotic manipulator. The actuator is capable of creating a local maximum magnetic field in a planar workspace, resulting in a convergence point in the influence zone. Therefore, the magnetic device is always trapped within this area during actuation. Figure 3f shows another actuator using two symmetrical permanent magnets with the angle between them adjusted by a linear mechanism.[48] This actuator creates both pushing and pulling forces along its axis of symmetry, and the positions of the separating points between the forward and reverse fields change with this angle. Connected with a robotic manipulator, this actuator performs satisfactory steering of the magnetic device in constrained environments. A system with three coaxial Halbach cylinders was also designed (Figure 3g). The inner ring has a pair of cylinders and each cylinder is composed of 16 magnets generating a strong uniform dipolar field. The outer ring contains one cylinder with eight magnets producing a graded quadrupolar field.[75] In this design, the component of the field gradient parallel to the dipolar field dominates the applied force; therefore, planner actuation is achieved by the rotational DOF of the inner ring. Dong et al. proposed a generic methodology using a spatially and temporally programmed external magnet array to control the configuration and the locomotion of the magnetic device (formations of collective magnetic microrobots), which sufficiently proves the versatility of magnetic field programming.[43]

3.2. Systems with Electromagnets

3.2.1. Paired Coils

A paired coil refers to a couple of electromagnets with obvious orthogonal distribution, and the workspace is at the central position. This type of magnetic actuation system often utilizes specialized coils as introduced in Section 2. The most common one is the multiaxial Helmholtz coil, which is composed of several Helmholtz coils, and the axis of each pair is mutually perpendicular to the others. **Figure 4**a shows a typical triaxial Helmholtz coil. According to the direct orthogonal decomposition of the magnetic field, this type of system can generate arbitrary magnetic fields with high uniformity in a plane (two Helmholtz coils) or space (three Helmholtz coils).[76–81] By appropriately setting the current flowing in each coil, a variety of magnetic fields are created, such as rotating, oscillating, alternating, and conical magnetic fields. Multiaxial square Helmholtz coils were also developed for other purposes, such as enlarging the inner space (Figure 4b).[49,82–84]

The Helmholtz coil is adept at torque control, and it can be incorporated with a Maxwell coil to execute force propulsion. Figure 4c shows a system containing a Helmholtz–Maxwell coil (one Helmholtz coil and one Maxwell coil assembled coaxially) that is installed on a rotational stage spinning about the center. In this system, the Helmholtz coil produces a uniform magnetic field to align the device, whereas the Maxwell coil creates a uniform field gradient for propulsion.[85,93] The propelling force is maintained parallel to the common axis, and 2D locomotion of the device is achieved by mechanical rotation. Similarly, Jeong et al. integrated two perpendicular Helmholtz–Maxwell coils for 3D locomotion (Figure 4d).[86] In this system, the inner Helmholtz–Maxwell coil is stationary and the outer Helmholtz–Maxwell coil can rotate along the horizontal axis. The frequency of the dynamic magnetic field is limited by inertia considering that both 1-DOF magnetic field and 1-DOF field gradient are provided by the rotational motion of coils. Yu et al. combined a triaxial Helmholtz coil with two Maxwell coils, as shown in Figure 4e.[87] A fixed Maxwell coil is at the outer side of the *z*-axial Helmholtz coil, and the other rotational Maxwell coil is rotated along the *z*-axis. This system can generate a high-frequency magnetic field and a restricted-frequency field gradient. Currently, these two systems have not fully realized 5-DOF control because the directions of the locomotion and orientation are coupled.

For electromagnetic systems using specialized coils, the currents flowing into the coils in a pair are interrelated; therefore, a pair of coils provides a 1-DOF magnetic component. There are some systems that use independently controlled paired coils, and such configurations are convenient for intuitional control and current computation.[94] For example, Floyd et al. proposed a system containing three independently controlled coil pairs (six coils) for 2D locomotion, in which horizontal coils are enabled to orient the device, and vertical coils are stimulated to steer the surface force (e.g., friction and adhesion that are pressure-related) (Figure 4f).[88] As a result, under the magnetic force exerted by the horizontal coils, the device can be propelled when the surface force is small and stopped when the surface force is large. Figure 4g shows a system using two independently controlled coil pairs (four coils) along the edges of a square, which can be used for both torque and force propulsion.[89,95–97] The created 2D magnetic field and field gradient are not as ideal as those created by specialized coils, but the discrepancy can be neglected or compensated in some situations. Leclerc et al. developed a magnetic actuation system using six coils in orthogonal pairs cooled with liquid nitrogen.[98] The current inside each coil is calculated to produce the desired field for orientation and the desired gradient for locomotion in 2D space, which can also be computed for other actuation strategies.[99]

The combination of Helmholtz coils and/or Maxwell coils has a low space efficiency considering the torso shape, which is not desirable due to scaling issues. For the sake of increasing

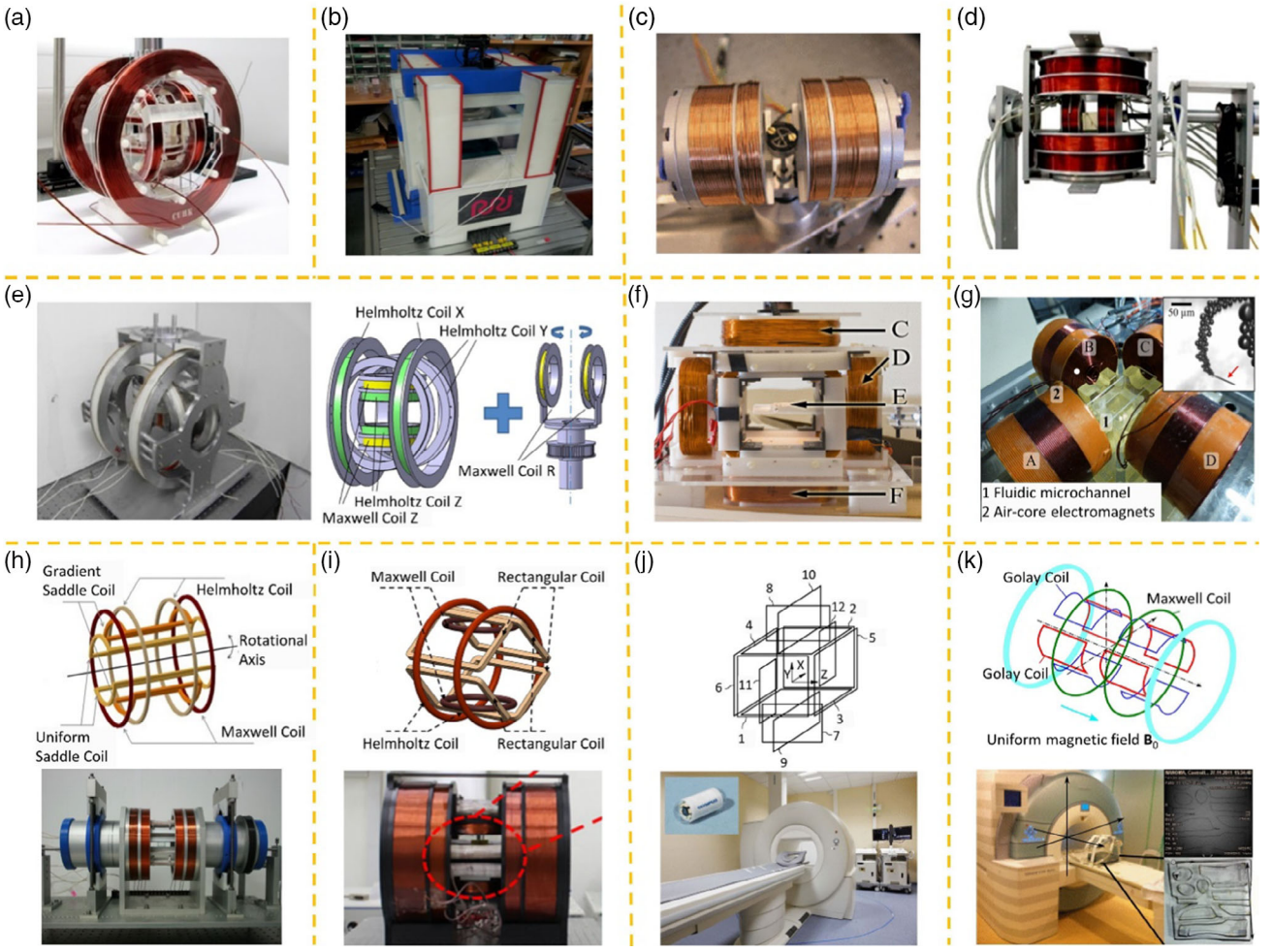

Figure 4. Magnetic actuation systems with paired coils: a) triaxial circular Helmholtz coil; b) triaxial square Helmholtz coil; c) system with a rotational Helmholtz–Maxwell coil; d) system using a stationary Helmholtz–Maxwell coil and a rotational Helmholtz–Maxwell coil; e) system consisting of a triaxial Helmholtz coil and two Maxwell coils; f) system using three independently controlled coil pairs; g) system comprising two independently controlled coil pairs; h) system with a Helmholtz coil, Maxwell coil, uniform saddle coil, and gradient saddle coil; i) system containing four independently controlled coil pairs; j) MGCE system; k) MRI scanner. Panel (b): Reproduced with permission.[84] Copyright 2011, Elsevier. Panel (c): Reproduced with permission.[85] Copyright 2007, IEEE. Panel (d): Reproduced with permission.[86] Copyright 2010, Elsevier. Panel (e): Adapted with permission.[87] Copyright 2010, Elsevier. Panel (f): Reproduced with permission.[88] Copyright 2009, IEEE. Panel (g): Adapted with permission.[89] Copyright 2014, IEEE. Panel (h): Adapted with permission.[27] Copyright 2010, Elsevier. Panel (i): Adapted with permission.[90] Copyright 2019, IEEE. Panel (j): Adapted with permission.[91] Copyright 2012, IEEE. Panel (k): Adapted with permission.[92] Copyright 2017, IEEE.

compactness and decreasing energy consumption, saddle coils have been included, and these systems usually have tubular constructions that suitably accommodate the human body. Choi et al. developed a system with four different coil pairs, among which the coaxial Helmholtz coil and Maxwell coil are fixed in the horizontal axis, and the coaxial uniform saddle coil and gradient saddle coil are rotatable along the horizontal axis (Figure 4h).[27] This system can be viewed as a variation from the system in Figure 4d. Later, the active locomotive intestinal capsule endoscope (ALICE) system with five coil pairs was developed by adding another uniform saddle coil based on the four-coil-pair system, so that three orthogonal coil pairs creating uniform magnetic fields (one Helmholtz coil and two uniform saddle coils) have the same function as a triaxial Helmholtz coil.[100] The actuation principle of ALICE is similar to the one shown in Figure 4e. To ensure high DOF locomotion and orientation with few coils, Go et al. proposed a system for 3D locomotion with four coils, consisting of two stationary circular coils (with the same configuration as the Helmholtz coil) and two rotatory saddle-shaped coils (with the same configuration as the uniform saddle coil).[56] All the currents are independently computed according to the required magnetic field and field gradient. Hoang et al. presented a tubular system with eight stationary coils distributed in four pairs (two pairs of circular coils and two pairs of rectangular coils evolved from saddle coils), which intends to maximize the workspace within a limited equipment volume.[90] Through independent current control, this system realizes 5-DOF orientation-independent actuation (Figure 4i).

Finally, two commercial magnetic actuation systems utilizing paired coils are introduced. Olympus Corporation (Tokyo, Japan)

and Siemens Healthineers AG (Erlangen, Germany) jointly developed the magnetically guided capsule endoscopy (MGCE) system, which consists of 12 coils (Figure 4g).[73,91,101] All the coils are in pairs, which are represented by consecutive numbers. Some coil pairs generate both magnetic field and field gradient components, whereas others create either a magnetic field or field gradient component. The system has been successfully evaluated in clinical trials with hundreds of patients and volunteers. The magnetic resonance imaging (MRI) scanner is a medical imaging tool that widely used in hospitals for diagnosis. It can generate an intense static uniform magnetic field in the horizontal axis and a dynamic 3D field gradient. Basically, a typical gradient coil unit in MRI scanner includes two orthogonal Golay coils and a Maxwell coil (Figure 4h).[92] Many researchers have applied MRI scanner for magnetic actuation, which has the potential for simultaneous actuation, localization, and imaging without introducing additional hardware.[102–105]

3.2.2. Distributed Electromagnets

Another branch of magnetic actuation systems utilizing distributed electromagnets has been developed to improve energy efficiency and mitigate layout restrictions. Most of the systems with paired coils tend to enclose the workspace via discal coils. In contrast, the distributed electromagnet-based systems usually have columnar coils positioning around and pointing to the workspace. Meanwhile, it is preferable to insert soft-iron cores into coils to concentrate and enhance the magnetic field and field gradient, which can be easily magnetized with the applied external magnetic field and rapidly demagnetized when the magnetic field disappears.

OctoMag is the first representative system with the configuration of a distributed array realizing 5-DOF wireless manipulation. It has eight identical electromagnets divided into two sets (**Figure 5**a).[28] Each electromagnet in the upper set has an angle of 45° with respect to the common axis of symmetry. We define this angle as the deflection that is applicable in the following description. The deflection of the lower set is 90°. Moreover, the upper set has a 45° rotation relative to the lower set along the common axis of symmetry. We regulate this angle as the misalignment, which also applies later. These design parameters are optimized to have sufficient force control capability throughout the workspace. Subsequently, MiniMag was redesigned from OctoMag, parameters of which are selected with the aim of high compactness, as shown in Figure 5b.[106] The optimized deflections of the two sets are 42.5° and 64°, respectively. Salmanipour et al. proposed a system with eight nonidentical electromagnets, whose parameters are defined to maximize the generated magnetic field and field gradient components (Figure 5c).[107] In this system, four electromagnets in the inner set have deflections of approximately 59.5°, four electromagnets in the outer set have deflections of 90°, and the misalignment is 45°. The radius of the outer electromagnet is more than twice that of the inner one. Son et al. developed a magnetic actuation system with nine electromagnets fixed in a 3×3 grid plate (Figure 5d).[14,108] The design parameters are optimized by the requirement of both actuation and localization. Four electromagnets have zero deflections, four have small deflections, and the added ninth electromagnet at the center is used to strengthen the magnetic field and field gradient toward the general direction.

The electromagnets in the aforementioned systems are arranged on one side of the central plane, meaning the workspace is semienclosed. The prominent feature is that such configurations are easy to integrate with the environment (e.g., OctoMag can be placed overhead while accommodating the head, neck, and shoulders). The uneven distribution is also convenient for combining with imaging and other devices. Another strategy is to arrange the electromagnets uniformly around the workspace for better isotropy of the generated magnetic field and field gradient. A typical system is shown in Figure 5e, whose upper set and lower set are positioned on the two sides of the central plane.[109] Each set has four orthogonal electromagnets with deflections of 45°, and a 45° misalignment exists between two sets. Figure 5f shows another system with a similar configuration, but the deflections of the two sets are both 60° to maximize separation and independence of the electromagnets.[110] There are also some systems whose upper set and lower set are directly facing, which means that the misalignment is zero. Le et al. designed a system with eight electromagnets placed in three dimensions at 90° with respect to one another, as shown in Figure 5g.[55] The eight electromagnets of the system in Figure 5h are arranged at each vertex of a cube and with each pointing to the center.[111]

As the electromagnets are controlled independently, the magnetic actuation system with eight (or more) well-arranged electromagnets should be capable of generating 8-DOF magnetic field and field gradient components without regardless of the singularity, so that the dexterity of magnetic actuation is guaranteed. Among the proposed configurations with eight electromagnets, it is not clear which one best configuration because a trade-off exists between force generation, torque generation, workspace isotropy, and access to the workspace, which was critically compared by Pourkand et al.[114] Rigorous quantification between the required number of stationary electromagnets and the given magnetic manipulation task was provided by Petruska et al, and this work systematically analyzed singularity issues under different circumstances.[39] Recently, a system with six orthogonal and identical electromagnets was developed, and the electromagnets are distributed from six vertices of a regular octahedron to the center (Figure 5i).[34] This system may not be as flexible as the preceding systems because of the reduced coil number, but it is characterized by an enlarged workspace.

The distributed electromagnet-based actuation system also has commercially available products. The Catheter Guidance Control and Imaging (CGCI) system developed by Magnetecs Corporation (California, USA) consists of eight electromagnets (Figure 5j).[112,115,116] Four electromagnets are semispherically arranged above the torso, and the other four are placed symmetrically below the torso. Aeon Scientific AG (Zurich, Switzerland) released the Aeon Phocus system with seven electromagnets fixed on two frames (one frame with four electromagnets and the other frame with three), as shown in Figure 5k.[113,117,118]. During operation, the electromagnets enclose the torso from both sides while performing magnetic actuation, and the two frames separate when enough space is required for medical imaging and surgeon intervention. These two systems are primarily targeted for magnetic catheter steering, but other tasks

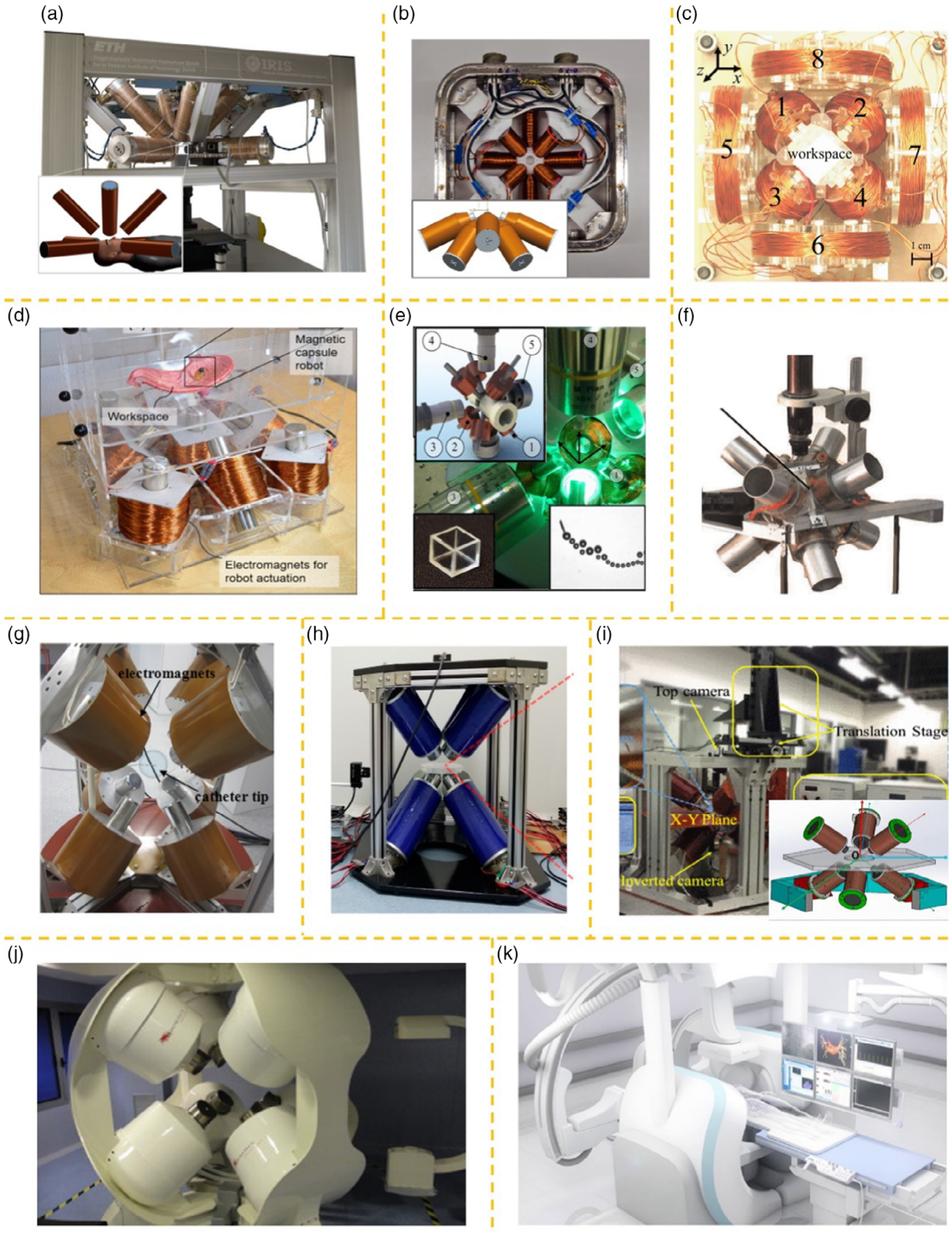

Figure 5. Magnetic actuation systems with stationary electromagnets: a) OctoMag system; b) MiniMag system; c) systems with an inner set and an outer set; d) system consisting of nine electromagnets; e) system having deflections of 45° and a misalignment of 45°; f) system with deflections of 60° and a misalignment of 45°; g) system comprising eight electromagnets placed in three dimensions at 90° angle with respect to one another; h) system using eight electromagnets distributed at each vertex of a cube; i) system consisting of six orthogonal electromagnets; j) CGCI system; k) Aeon Phocus system. Panel (a): Adapted with permission.[28] Copyright 2010, IEEE. Panel (b): Adapted with permission.[106] Copyright 2014, Springer Nature. Panel (c): Reproduced with permission.[107] Copyright 2018, IEEE. Panel (d): Reproduced with permission.[108] Copyright 2019, IEEE. Panel (e): Adapted with permission.[109] Copyright 2013, AIP. Panel (f): Reproduced with permission.[110] Copyright 2014, Wiley-VCH. Panel (g): Reproduced with permission.[55] Copyright 2016, Wiley. Panel (h): Reproduced under the terms of the CC BY 4.0 license.[111] Copyright 2019, The Authors, published by MDPI. Panel (i): Adapted with permission.[34] Copyright 2017, IEEE. Panel (j): Reproduced with permission.[112] Copyright 2013, Elsevier. Panel (k): Reproduced under the terms of the CC BY 4.0 license.[113] Copyright 2019, The Authors, published by Wiley-VCH.

can also be performed. Currently, they have been CE certified and have shown promising results in animal experiments and clinical assessments.

Apart from the systems with stationary electromagnets, transformable ones have also been developed. The actuation systems with different configurations perform diversely considering magnetic actuation manipulability and dexterity: some are superior in force control, and others have better performance at torque control.[58] Moreover, singularities may exist for some systems, which means that the systems will lose the ability to generate certain force/torque at the singularity or cost a lot near the singularity, but the actuation should be comprehensive.[119] In view of these factors, adjustable magnetic actuation systems have been proposed. BigMag contains six electromagnets placed in two fixtures. The upper and lower fixtures are capable of rotating around the common axis to avoid singularity and minimize the total current, so that the system can generate a strong magnetic field in any direction and at any point of the workspace (**Figure 6**a).[54,57] The intersection angle between two adjacent electromagnets is 60° when all the electromagnets are coplanar. Chen et al. proposed a system comprising four stationary and four movable electromagnets (Figure 6b).[120] The construction of this system is similar to that of OctoMag, but the deflections of the upper set are independently adjusted by robotic mechanisms, which leads to the problem of prioritizing between the uniform magnetic field and the uniform field gradient.

To enlarge the workspace further without increasing the size of electromagnets, driven mechanisms have been introduced to locate the mobile electromagnets near the ROI. The advanced robotics for magnetic manipulation (ARMM) system connects an optimized cylindrical electromagnet with a 6-DOF UR10 robotic arm (produced by Universal Robots), which is capable of creating

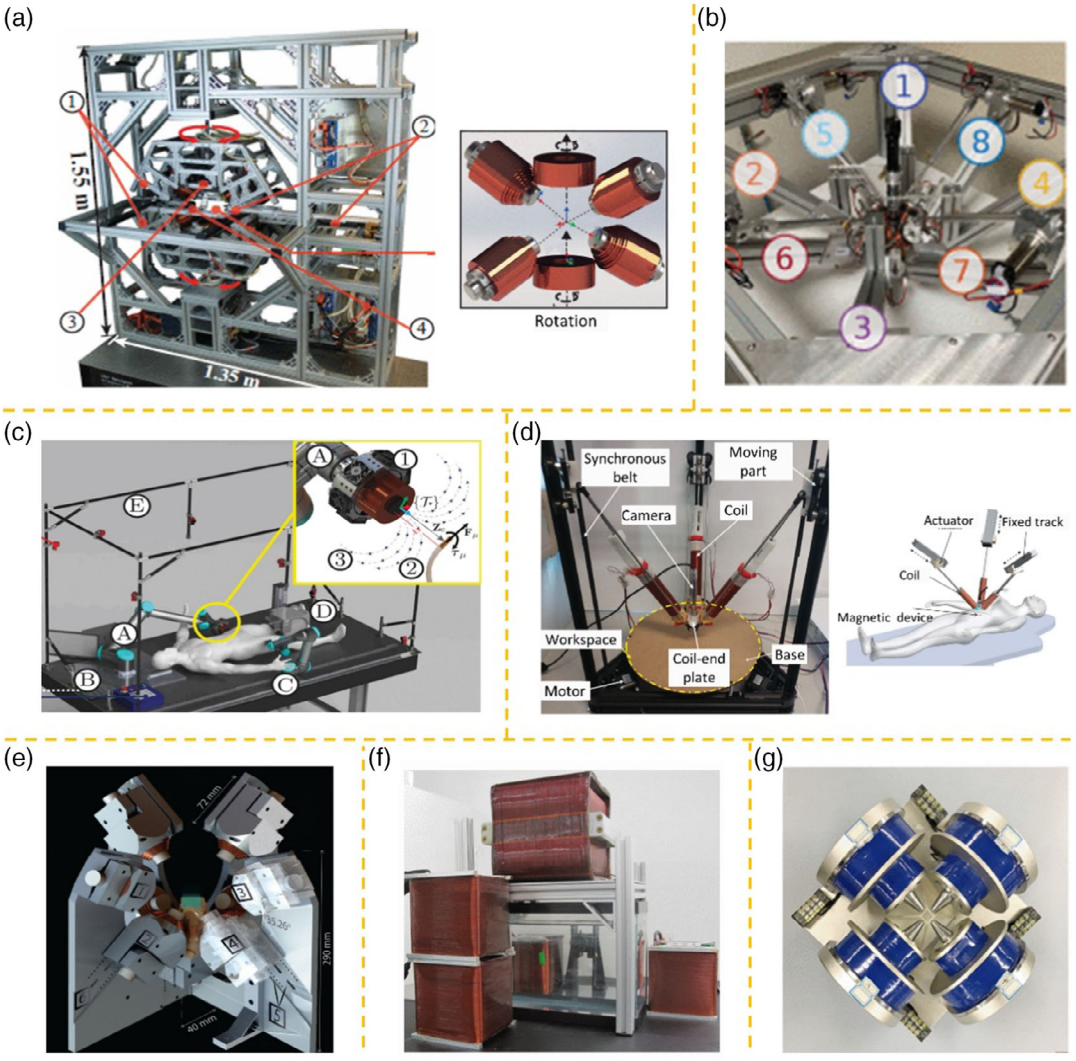

Figure 6. Magnetic actuation systems with movable electromagnets or novel designs: a) BigMag system; b) system with four stationary and four movable electromagnets; c) ARMM system; d) DeltaMag system; e) BatMag system; f) Omnimagnet system; g) system comprising stepped cores. Panel (a): Adapted with permission.[54] Copyright 2017, IEEE. Panel (b): Reproduced with permission.[120] Copyright 2019, IEEE. Panel (c): Reproduced with permission.[121] Copyright 2019, IEEE. Panel (d): Adapted with permission.[122] Copyright 2019, IEEE. Panel (e): Reproduced with permission.[123] Copyright 2019, IEEE. Panel (f): Reproduced with permission.[124] Copyright 2015, IEEE. Panel (g): Reproduced with permission.[35] Copyright 2020, IEEE.

a prescribed magnetic field and field gradient at the ROI (Figure 6c).[121,125] This concept was also implemented using a U-shape electromagnet by Lucarini et al.[126] Instead of designing an electromagnetic actuator for a commercial robotic arm, DeltaMag integrated three electromagnets into a parallel mechanism, as shown in Figure 6d. The unique design effectively enlarges the workspace and reduces the total volume, which has the potential to be further combined with an in vivo locating device.[122] Although moveable electromagnetic systems have various merits, great challenges still exist. Different from the permanent magnet, the electromagnet has a relatively large volume and weight; in addition, a multicoil configuration that has strong interaction forces is necessary for some situations. Therefore, integrating reliable-driven mechanisms with enough load capability, high rigidity, and good structural compactness is essential. In addition, multiple solutions and high nonlinearities may exist due to total DOF of both driven mechanisms and coil currents, so developing field generation algorithms with good robustness, fast speed, and optimal characteristics needs further explorations.

Finally, some novel designs are presented. Ongaro et al. devised BatMag with nine electromagnets (Figure 6e), which can independently control two devices in a 3D space exploiting the inhomogeneity of the strong fields.[123] Figure 6f shows a modular and reconfigurable magnetic actuation system containing multiple Omnimagnets, which can be momentarily rearranged during actuation.[30,124] Each Omnimagnet comprises a spherical core and three orthogonally surrounding nested solenoids, and the magnetization of the core is determined by the currents in three solenoids. Li et al. developed a system with four electromagnets, each of which has a stepped core with a cone probe and a disk (Figure 6g).[35] The optimized core shape is used to further enhance the strength of the magnetic field and field gradient.

4. Magnetic End Effectors

Magnetic actuation can be imposed on diverse miniature robots, which are considered as end effectors of the aforementioned systems. These miniature agents are introduced in accordance with their characteristics and present usage (**Figure 7**). Moreover, the current and potential biomedical applications of controllable end effectors are summarized.

4.1. Overview of End Effectors

4.1.1. Continuum End Effectors

Catheters have been used in clinics to treat vascular diseases. However, conventional procedures highly depend on the experience of the surgeon, which are still risky and time-consuming. Magnetic actuation is an alternative method with higher precision and less radiation. Magnetically controlled catheters are equipped with various magnetic components, the most popular of which is the permanent magnet, which is capable of importing obvious responses to the magnetic field owing to the large residual magnetization. Both single magnet and multiple magnets are embedded on the tip of catheters, so that these flexible devices bend upon the induced magnetic torque and/or force.[55,127–129] The relative stiffness of the catheter changes during insertion, to figure out the nonlinearity and uncertainty, a catheter with a tethered magnet was designed to allow accurate computation of the distal end.[117] Mounting the ferromagnetic sphere is another option, and this type of catheter is often actuated by the applied magnetic gradient.[130,131] Recently, a catheter fabricated from magnetized ink composed of hard magnetic particles and soft polymer was devised, and its diameter can be miniaturized below hundreds of micrometers.[12] Catheters with controllable magnetization have also been proposed. These are mainly used in MRI scanners in view of the static uniform magnetic field, as mentioned in Section 3. A solenoid with magnetization proportional to the flowing current is attached to the tip of the catheter, so that the generated magnetic torque is controllable.[132,133] Nevertheless, the singularity is severe, considering the constant magnetized direction. On account of this limitation, the catheter with multiple coils has been proposed.[38] The diameter of the coil-based catheter has the potential to be decreased by micromachining.

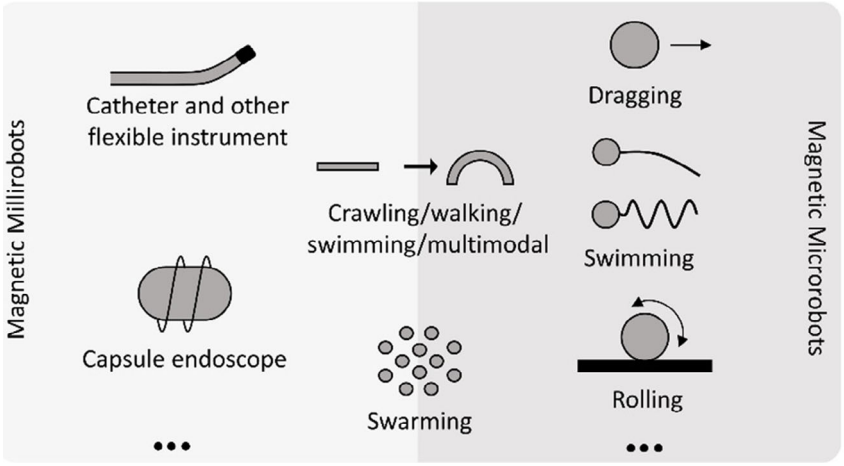

Figure 7. Typical magnetic miniature end effectors including continuum and untethered robots.

The magnet actuation of other flexible instruments going through the lumens and ducts of the body has also received attention for better maneuverability, such as needles and continuum endoscopes.[113,134–137] The steering of these magnetic continuum manipulators is basically similar: forward and reversed feeding is provided by proximal insertion (manual or mechanical), and distal tip deflection is controlled by the applied magnetic effect.

4.1.2. Untethered End Effectors

The capsule endoscope is widely developed for examination and diagnosis in the GI tract. Aiming at more comprehensive screening and short duration, both completely untethered and soft-wire tethered (almost have no influence on motion and thus are included in the untethered classification) magnetic capsules are proposed, most of which are embedded with the permanent magnet.[61,65,138] The magnetic capsule, whose locomotion results from the drag force exerted by the field gradient, has been applied in hospitals for the past few years.[67,91] Another type of propulsion uses the applied magnetic torque. Examples include fish-like capsules actuated by an alternating magnetic field[139] and spiral-type capsules actuated by a rotating magnetic field.[140] More details of the magnetic capsule endoscopy can be found from a survey by shamsudhin et al.[21]

Multifold magnetic microrobots, which have the ability to access extremely narrow regions, have been invented and demonstrated. Knowing their motion modality is useful in selecting an appropriate end effector for the chosen actuation system, or building an adaptive actuation system to propel a targeted end effector. As the most straightforward strategy, dragging microrobots with the propulsive force resulting from a field gradient are proposed.[28,141] Inspired by biological microorganisms, torque-driven swimming microrobots are developed, such as screw-like microrobots mimicking bacteria[142–145] and flexible oar-like microrobots imitating spermatozoa.[146] These two types of robots can realize 3D locomotion. The movement of rolling microrobots is caused by uneven boundary conditions, which is only valid near the surface.[94,147,148] An apparent viscosity increment occurs when the microrobot rotates near the surface, and the unbalanced force leads to locomotion. Other surface walkers have also been developed.[149,150] Note that both screw-like swimming microrobots and rolling microrobots can be driven by a rotating magnetic field. However, the moving directions are different: the former propels along the rotating axis, whereas the latter advances along the rotating surface. Another type of locomotion is often bionic and triggered by deformations of robots. Examples include insect-like crawling,[151] multilegged walking,[152] and jellyfish-like swimming.[153] Soft-bodied robots constructed of active materials with multimode locomotion were proposed to realize high mobility on different terrains, whose motion pattern is switched by exerting different magnetic fields.[154] Except for triggered locomotion, the fast shape transformation of soft magnetic robots itself is noteworthy, which achieves more functions.[155] These robots are fabricated by soft materials embedded with ferromagnetic or paramagnetic micro/nanoparticles, various deformations of which are fulfilled by programmable structures and magnetization profiles while applying external magnetic fields.[156,157]

Apart from the individually locomotor microrobots, swarming robots have been designed. Governed by the magnetic field, agent–agent effect, fluidic force, and other interactions, a group of micro/nanorobots can be dynamically assembled into snake-like,[95] vortex-like,[158] ribbon-like, and other patterns,[159] and can move as a relatively stable unit. Some swarming robots are reconfigurable to adapt to various situations[160,161] and have the potential to enhance medical imaging.[162,163]

4.2. Biomedical Applications

The good controllability and small dimensions enable magnetic end effectors to locomote in complex and confined environments, leading to their current and potential biomedical applications (**Figure 8**). Optical imaging is a significant method for clinical examination. Direct and comprehensive visualization of the GI tract, vasculature, lung, and other lumens and ducts can be achieved using end effectors with miniature cameras.[67,135] Biopsy is also commonly utilized in the clinic that extracts sample cells or tissues from the body for further tests. Magnetic miniature robots provide less-invasive options, for example, millimeter end effectors integrated with tiny forceps and needles[14] and micrometer end effectors such as responsive microgrippers.[164] Biomedical sensing can detect medically relevant factors, including pH, oxygen, virus, and bacteria, which offer evidences for diagnoses. The sensor with mobility may access to a specific location of the human body and conduct in situ sensing.[165] In addition, the autonomous motion of a functionalized microrobot can accelerate the procedure of in vitro detection.[166] Some miniature robots can be precisely actuated near the target position and release carried substances. This process is targeted delivery, which is an effective method for improving accessibility and concentration of the cargo at the ROI and reduces side effects on normal organs.[5] The potential cargo for delivery covers drugs, genes, stem cells, and imaging agents.[167,168] In addition to the mentioned diagnostic and therapeutic functions, miniature robots also possess the ability to perform minimally invasive surgeries. Some continuum end effectors have successfully demonstrated surgical operations, such as atrial fibrillation ablation and percutaneous coronary intervention.[23] Untethered end effectors are good candidates for performing surgery (e.g., thrombolysis, hyperthermia, and cauterization) at some hard-to-reach regions.[169–171]

Cell manipulation, which is an effective method of learning tissue regeneration, drug development, single-cell analysis, and intercellular interaction, can be accomplished by these end effectors. Remotely actuated microrobots can separate a cell from a population, transport a cell in sophisticated surroundings, and release a cell at a target location.[16,173] Micro end effectors are also strong performers in tissue engineering. The end effector itself can be fabricated into a scaffold, providing a frame for tissue regeneration, whose mobility also supports further transplantation.[172] Alternatively, the end effector can deploy microbuilding blocks into a desired geometry, and the whole structure acts as a scaffold.[174]

It is worth noting that the micromagnetofluidics provides an effective and efficient choice for lab-on-a-chip applications, which is a technology combining magnetism with microfluidics.[175,176]

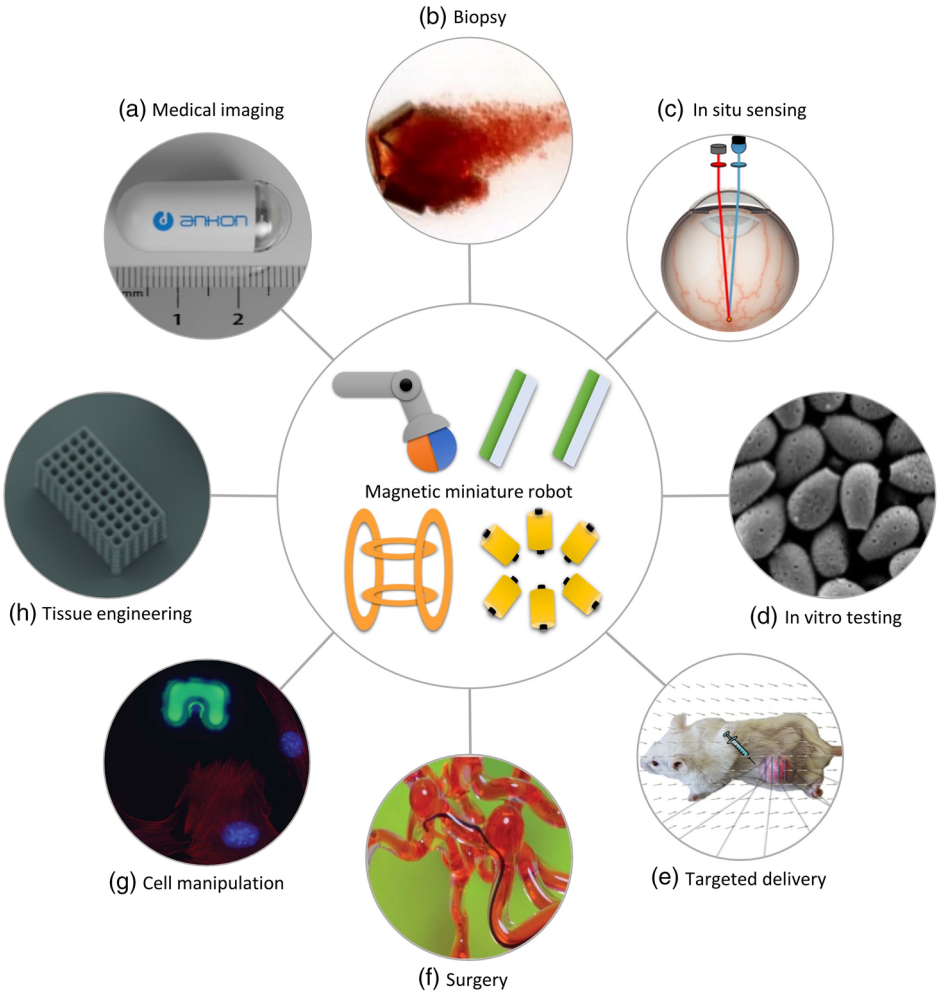

Figure 8. Medical and bioengineering applications of magnetic end effectors: a) magnetic capsule endoscopy produced by Ankon Technologies for imaging; b) magnetic microgrippers for biopsy; c) magnetic and optical oxygen sensor for in situ intraocular sensing; d) magnetic spore-based microrobots that remotely detect toxins for in vitro testing; e) swarms of magnetotactic bacteria for targeted delivery; f) ferromagnetic soft continuum robot for surgery; g) autofluorescent magnetic microrobots for single-cell manipulation; h) magnetic scaffold to culture cells for tissue engineering. Panel (a): Reproduced with permission.[67] Copyright 2016, Elsevier. Panel (b): Reproduced with permission.[164] Copyright 2009, NAS. Panel (c): Adapted with permission.[165] Copyright 2008, IEEE. Panel (d): Reproduced with permission.[166] Copyright 2019, AAAS. Panel (e): Reproduced with permission.[10] Copyright 2016, Springer Nature. Panel (f): Reproduced with permission.[12] Copyright 2019, AAAS. Panel (g): Reproduced with permission.[16] Copyright 2013, SAGE. Panel (h): Reproduced with permission.[172] Copyright 2011, Wiley-VCH.

The external magnetic field offers wireless manipulation, and the microfluidics reduces the number of samples and enables high throughput. One of the significant applications is the droplet-based microfluidic device, where ferrofluid and magnetic beads are often adopted, which is versatile in single-cell manipulation and biological macromolecule characterization.[177,178] Common microfluidic functions, such as pumping and mixing, are also performable through magnetic methods.[175]

5. Conclusions

A controllable magnetic field is a powerful tool for remote actuation, which fulfills the locomotion of magnetic miniature robots in intricate and confined environments. Accordingly, the performance of the magnetic actuation system directly affects ultimate applications. The initial concept of controlling the magnetic field involves spatial variations of a permanent magnet and different combinations of electromagnetic currents. Some possible advantages and disadvantages of typical mobile permanent magnetic systems and stationary electromagnetic systems are shown in **Table 1**. Each category has its own merits, and the features between the two types are partly complementary. Recently, some novel systems have been designed to combine the advantages of both types. For example, the permanent magnetic system with a spherical actuator (Figure 2d) and with eight independent rotary magnets (Figure 3d) can realize high dexterity of field generation, mitigated complexity and perilousness of motion, and no heat generation. With regard to the electromagnetic system, the ARMM system (Figure 6c)

Table 1. Some possible advantages and disadvantages of the most common configurations of magnetic actuation systems.

Configuration	Advantages	Disadvantages
Mobile permanent magnets	Adjustable size of workspace	Partial dexterity of field generation
	Strong magnetic field without heating effect	Magnetic field cannot be turned off
	Good environmental adaptability	Complex motion control algorithm
Stationary electromagnets	Comprehensive ability of field generation	Difficult to scale up
	On/off manipulability of magnetic field	Energy consumption and heat production
	Simple current control strategy	Poor environmental adaptability

and the DeltaMag system (Figure 6d) possess enlarged workspaces with reduced heat generation, on/off manipulability of the magnetic field, and suitable accommodation with imaging devices. Development and selection of magnetic actuation systems are case-by-case, which require an overall consideration of the field generation ability, computational difficulty, working scenario, and cost performance.

The future focus on magnetic actuation systems may be fourfold, most of which mainly concentrate on medical applications. First is the scaling issue, which is prominent for electromagnetic systems. The magnetic field and field gradient attenuate rapidly with the distance; therefore, a larger workspace usually requires bulkier electromagnets and higher currents. Cooling systems, such as forced air cooling,[121] water cooling,[127] liquid nitrogen cooling,[98] and superconducting,[179] are necessary to accelerate the dissipation of resistive heat and mitigate heat effect. Another option is to use mobile electromagnets that can approach the ROI, as reported recently.

Second is the integration with imaging devices at the system level. Imaging devices (e.g., optical microscopes and cameras) are mostly positioned at the interspace of the actuation system for in vitro applications, and this arrangement is generally accepted. Concerning in vivo applications, imaging remains a challenge.[180] Magnetic localization is a good candidate for millimeter end effectors but arduous for micrometer end effectors. Using MRI for simultaneous actuation, localization, and imaging is another solution, but patients with cardiac pacemakers and metallic foreign bodies are excluded. Fluoroscopy equipment has a strict requirement of free space, and radiation is inevitable. Translational and rotational movements of the probe are necessary during ultrasound imaging, which need to be solved when integrated with magnetic actuation systems.

Third is safety considerations. Medical equipment hazards may threaten both patients and medical staff; therefore, ensuring safety is one of the critical issues. For example, a robotic arm working near the body should always conduct high-precision collision-free motion, the security of the strong magnetic field needs to be guaranteed, and the safety and effectiveness of the cooling system must be maintained.

Fourth is improving the performance of the applied magnetic field. The high-frequency magnetic field, which is necessary for some situations (usually less than 150 Hz),[181] is hard to be produced due to bandwidth limitation. For the permanent magnetic system, the inertia confines the physical motion of the mechanism. Regarding the electromagnetic actuation system, multiturn copper wire results in strong induction, and the hysteresis of the soft-iron core also has an inevitable effect, both of which are ignored at low frequency but need to be compensated at high frequency. Another issue is magnetic field inaccuracy caused by heat effect, which needs to be addressed for the generation of highly precise magnetic fields.

In summary, this survey reviews the state-of-the-art magnetic actuation systems, including the basic theory, systematic configuration, biomedical applications, and potential challenges. Although some newly proposed magnetic actuation systems still claim further development and validation, the preliminary results have satisfactorily demonstrated the improved controllability of magnetic end effectors for diverse applications. Combined with multifunctional miniature robots, advanced control methods, and other technologies, magnetic actuation systems will allow significant advances in biomedical innovations.

Acknowledgements

The authors acknowledge funding support from the Hong Kong University Grants Committee (RGC) under GRF Project (no. 14218516) and JLFS Project (no. JLFS/E- 402/18), the Hong Kong Innovation and Technology Commission (ITC) under ITF Projects (MRP/036/18X and ITS/374/18FP), and the Chinese University of Hong Kong (CUHK) under Research Sustainability of Major RGC Funding Schemes (RSFS) (no. 3133228) and the Direct Grant (no. 4055111).

Conflict of Interest

The authors declare no conflict of interest.

Keywords

biomedical applications, magnetic actuation, medical robots and systems, microrobots, miniature robots

Received: April 20, 2020
Revised: May 12, 2020
Published online: June 24, 2020

[1] K. E. Peyer, L. Zhang, B. J. Nelson, *Nanoscale* **2013**, *5*, 1259.
[2] J. Li, B. E. F. de Ávila, W. Gao, L. Zhang, J. Wang, *Sci. Robot.* **2017**, *2*, eaam6431.
[3] M. Medina-Sánchez, O. G. Schmidt, *Nature* **2017**, *545*, 406.
[4] S. Palagi, P. Fischer, *Nat. Rev. Mater.* **2018**, *3*, 113.
[5] M. Sitti, *Nat. Rev. Mater.* **2018**, *3*, 74.
[6] G. Z. Yang, J. Bellingham, P. E. Dupont, P. Fischer, L. Floridi, R. Full, N. Jacobstein, V. Kumar, M. McNutt, R. Merrifield, B. J. Nelson, B. Scassellati, M. Taddeo, R. Taylor, M. Veloso, Z. L. Wang, R. Wood, *Sci. Robot.* **2018**, *3*, eaar7650.
[7] M. Sitti, H. Ceylan, W. Hu, J. Giltinan, M. Turan, S. Yim, E. Diller, *Proc. IEEE* ***2015***, *103*, 205.

[8] B. J. Nelson, I. K. Kaliakatsos, J. J. Abbott, *Annu. Rev. Biomed. Eng.* **2010**, *12*, 55.
[9] S. Jeon, S. Kim, S. Ha, S. Lee, E. Kim, S. Y. Kim, S. H. Park, J. H. Jeon, S. W. Kim, C. Moon, B. J. Nelson, J. Y. Kim, S. W. Yu, H. Choi, *Sci. Robot.* **2019**, *4*, eaav4317.
[10] O. Felfoul, M. Mohammadi, S. Taherkhani, D. de Lanauze, Y. Zhong Xu, D. Loghin, S. Essa, S. Jancik, D. Houle, M. Lafleur, L. Gaboury, M. Tabrizian, N. Kaou, M. Atkin, T. Vuong, G. Batist, N. Beauchemin, D. Radzioch, S. Martel, *Nat. Nanotechnol.* **2016**, *11*, 941.
[11] S. Lee, S. Lee, S. Kim, C. H. Yoon, H. J. Park, J. y. Kim, H. Choi, *Sci. Rep.* **2018**, *8*, 3691.
[12] Y. Kim, G. A. Parada, S. Liu, X. Zhao, *Sci. Robot.* **2019**, *4*, eaax7329.
[13] S. Yim, E. Gultepe, D. H. Gracias, M. Sitti, *IEEE Trans. Biomed. Eng.* **2013**, *61*, 513.
[14] D. Son, H. Gilbert, M. Sitti, *Soft Robot.* **2019**, *7*, 10.
[15] E. W. Jager, O. Inganäs, I. Lundström, *Science* **2000**, *288*, 2335.
[16] E. B. Steager, M. Selman Sakar, C. Magee, M. Kennedy, A. Cowley, V. Kumar, *Int. J. Robot. Res.* **2013**, *32*, 346.
[17] H. Ceylan, J. Giltinan, K. Kozielski, M. Sitti, *Lab Chip* **2017**, *17*, 1705.
[18] G. Kosa, P. Hunziker, *Adv. Intell. Syst.* **2019**, *1*, 1900035.
[19] P. Fischer, A. Ghosh, *Nanoscale* **2011**, *3*, 557.
[20] T. Xu, J. Yu, X. Yan, H. Choi, L. Zhang, *Micromachines* **2015**, *6*, 1346.
[21] N. Shamsudhin, V. I. Zverev, H. Keller, S. Pane, P. W. Egolf, B. J. Nelson, A. M. Tishin, *Med. Phys.* **2017**, *44*, e91.
[22] C. Heunis, J. Sikorski, S. Misra, *IEEE Robot. Autom. Mag.* **2018**, *25*, 71.
[23] J. Hwang, J. Y. Kim, H. Choi, *Intell. Serv. Robot. 2020*, 13, 1.
[24] X. Z. Chen, M. Hoop, F. Mushtaq, E. Siringil, C. Hu, B. J. Nelson, S. Pané, *Appl. Mater. Today* **2017**, *9*, 37.
[25] M. F. McCaslin, *Trans. Am. Ophthalmol. Soc.* **1958**, *56*, 571.
[26] A. Heilbronn, *Jahrb. Wiss. Bot.* **1922**, *61*, 284.
[27] H. Choi, K. Cha, J. Choi, S. Jeong, S. Jeon, G. Jang, J. O. Park, S. Park, *Sens. Actuators A* **2010**, *163*, 410.
[28] M. P. Kummer, J. J. Abbott, B. E. Kratochvil, R. Borer, A. Sengul, B. J. Nelson, *IEEE Trans. Robot.* **2010**, *26*, 1006.
[29] A. W. Mahoney, J. J. Abbott, *IEEE Trans. Robot.* **2013**, *30*, 411.
[30] A. J. Petruska, J. J. Abbott, *IEEE Trans. Magn.* **2014**, *50*, 1.
[31] A. Zarrouk, K. Belharet, O. Tahri, A. Ferreira, in *IEEE Int. Conf. Robotics and Automation*, IEEE, Montreal **2019**, p. 883.
[32] L. Yang, E. Yu, C. Vong, L. Zhang, *IEEE/ASME Trans. Mechatron.* **2019**, *24*, 1208.
[33] A. Oulmas, N. Andreff, S. Régnier, *Int. J. Robot. Res.* **2018**, *37*, 1359.
[34] F. Niu, J. Li, W. Ma, J. Yang, D. Sun, *IEEE/ASME Trans. Mechatron.* **2017**, *22*, 2265.
[35] D. Li, F. Niu, J. Li, X. Li, D. Sun, *IEEE Trans. Ind. Electron. 2020*, 67, 4700.
[36] E. Diller, J. Giltinan, G. Z. Lum, Z. Ye, M. Sitti, *Int. J. Robot. Res.* **2016**, *35*, 114.
[37] L. Yang, Y. Zhang, Q. Wang, K. Chan, L. Zhang, *IEEE Trans. Autom. Sci. Eng. 2020*, 17, 490.
[38] T. Greigarn, R. Jackson, T. Liu, M. C. Çavuşoğlu, in *IEEE Int. Conf. Robotics and Automation*, IEEE, Singapore **2017**, p. 3600.
[39] A. J. Petruska, B. J. Nelson, *IEEE Trans. Robot.* **2015**, *31*, 714.
[40] E. P. Furlani, *Permanent Magnet and Electromechanical Devices: Materials, Analysis, and Applications*, Academic Press, Cambridge, MA **2001**.
[41] C. R. Thornley, L. N. Pham, J. J. Abbott, *IEEE Robot. Autom. Lett.* **2019**, *4*, 2325.
[42] A. J. Petruska, J. J. Abbott, *IEEE Trans. Magn.* **2013**, *49*, 811.
[43] X. Dong, M. Sitti, *Int. J. Robot. Res.* **2020**, *39*, 617.
[44] J. J. Abbott, E. Diller, A. J. Petruska, *Annu. Rev. Control Robot. Autom. Syst.* **2019**, *3*, 57.
[45] A. W. Mahoney, J. J. Abbott, *Int. J. Robot. Res.* **2016**, *35*, 129.
[46] P. Ryan, E. Diller, *IEEE Trans. Robot.* **2017**, *33*, 1398.
[47] M. E. Alshafeei, A. Hosney, A. Klingner, S. Misra, I. S. M. Khalil, in *IEEE RAS/EMBS Int. Conf. Biomedical Robotics and Biomechatronics*, IEEE, Sao Paulo **2014**, p. 151.
[48] W. Amokrane, K. Belharet, M. Souissi, A. B. Grayeli, A. Ferreira, *Robot. Auton. Syst.* **2018**, *107*, 10.
[49] Y. H. Ha, B. H. Han, S. Y. Lee, *Med. Biol. Eng. Comput.* **2010**, *48*, 139.
[50] D. M. Ginsberg, M. J. Melchner, *Rev. Sci. Instrum.* **1970**, *41*, 122.
[51] S. Jeon, G. Jang, H. Choi, S. Park, *IEEE Trans. Magn.* **2010**, *46*, 1943.
[52] C. E. G. Salmon, E. L. G. Vidoto, M. J. Martins, A. Tannús, *Braz. J. Phys.* **2006**, *36*, 4.
[53] S. S. Hidalgo-Tobon, *Concepts Magn. Reson. A* **2010**, *36A*, 223.
[54] J. Sikorski, I. Dawson, A. Denasi, E. E. Hekman, S. Misra, in *IEEE Int. Conf. Robotics and Automation*, IEEE, Singapore **2017**, p. 3594.
[55] V. N. T. Le, N. H. Nguyen, K. Alameh, R. Weerasooriya, P. Pratten, *Med. Phys.* **2016**, *43*, 650.
[56] G. Go, H. Choi, S. Jeong, C. Lee, S. Y. Ko, J. Park, S. Park, *IEEE Trans. Magn.* **2015**, *51*, 1.
[57] J. Sikorski, A. Denasi, G. Bucchi, S. Scheggi, S. Misra, *IEEE/ASME Trans. Mechatron.* **2019**, *24*, 505.
[58] R. Chen, D. Folio, A. Ferreira, in *IEEE Int. Conf. Robotics and Automation*, IEEE, Montreal **2019**, p. 2474.
[59] W. Andrä, H. Nowak, *Magnetism in Medicine: A Handbook*, John Wiley & Sons, **2007**.
[60] J. Patrick Reilly, *Health Phys.* **2014**, *107*, 343.
[61] G. Ciuti, P. Valdastri, A. Menciassi, P. Dario, *Robotica* **2010**, *28*, 199.
[62] G. Ciuti, R. Donlin, P. Valdastri, A. Arezzo, A. Menciassi, M. Morino, P. Dario, *Endoscopy* **2010**, *42*, 148.
[63] P. Valdastri, G. Ciuti, A. Verbeni, A. Menciassi, P. Dario, A. Arezzo, M. Morino, *Surg. Endosc.* **2012**, *26*, 1238.
[64] S. Tognarelli, V. Castelli, G. Ciuti, C. Di Natali, E. Sinibaldi, P. Dario, A. Menciassi, *J. Robot. Surg.* **2012**, *6*, 5.
[65] G. Pittiglio, L. Barducci, J. W. Martin, J. C. Norton, C. A. Avizzano, K. L. Obstein, P. Valdastri, *IEEE Robot. Autom. Lett.* **2019**, *4*, 1224.
[66] S. E. Wright, A. W. Mahoney, K. M. Popek, J. J. Abbott, *IEEE Trans. Robot.* **2017**, *33*, 1013.
[67] Z. Liao, X. Hou, E. Q. Lin-Hu, J. Q. Sheng, Z. Z. Ge, B. Jiang, X. H. Hou, J. Y. Liu, Z. Li, Q. Y. Huang, *Clin. Gastroenterol. Hepatol.* **2016**, *14*, 1266.
[68] S. Yim, M. Sitti, *IEEE Trans. Robot.* **2012**, *28*, 183.
[69] M. T. Hou, H. M. Shen, G. L. Jiang, C. N. Lu, I. J. Hsu, J. A. Yeh, *Appl. Phys. Lett.* **2010**, *96*, 024102.
[70] T. W. R. Fountain, P. V. Kailat, J. J. Abbott, in *IEEE Int. Conf. Robotics and Automation*, IEEE, Anchorage, AK **2010**, p. 576.
[71] J. S. Lee, B. Kim, Y. S. Hong, *Int. J. Precis. Eng. Manuf.* **2009**, *10*, 27.
[72] M. P. Armacost, J. Adair, T. Munger, R. R. Viswanathan, F. M. Creighton, D. T. Curd, R. Sehra, *J. Cardiovasc. Electrophysiol.* **2007**, *18*, S26.
[73] F. Carpi, C. Pappone, *Expert Rev. Med. Devices* **2009**, *6*, 487.
[74] W. Zhang, Y. Meng, P. Huang, *IEEE Trans. Magn.* **2008**, *44*, 2367.
[75] O. Baun, P. Blümler, *J. Magn. Magn. Mater.* **2017**, *439*, 294.
[76] A. W. Mahoney, J. C. Sarrazin, E. Bamberg, J. J. Abbott, *Adv. Robot.* **2011**, *25*, 1007.
[77] T. Xu, G. Hwang, N. Andreff, S. Régnier, *IEEE Trans. Robot.* **2015**, *31*, 117.
[78] C. Huang, T. Xu, J. Liu, L. Manamanchaiyaporn, X. Wu, *IEEE Robot. Autom. Lett.* **2019**, *4*, 4185.
[79] L. Yang, Q. Wang, L. Zhang, *IEEE Trans. Nanotechnol.* **2018**, *17*, 697.
[80] A. Denasi, F. Khan, K. J. Boskma, M. Kaya, C. Hennersperger, R. Göbl, M. Tirindelli, N. Navab, S. Misra, in *IEEE Int. Conf. Robotics and Automation*, IEEE, Brisbane **2018**, p. 50.
[81] J. Yu, L. Zhang, *IEEE/ASME Trans. Mechatron.* **2019**, *24*, 154.
[82] D. Byun, J. Choi, K. Cha, J. O. Park, S. Park, *Mechatronics* **2011**, *21*, 357.

[83] S. H. Kim, K. Ishiyama, *IEEE/ASME Trans. Mechatron.* **2013**, *19*, 1651.
[84] S. Jeong, H. Choi, K. Cha, J. Li, J. O. Park, S. Park, *Sens. Actuators A* **2011**, *171*, 429.
[85] J. J. Abbott, Z. Nagy, F. Beyeler, B. J. Nelson, *IEEE Robot. Autom. Mag.* **2007**, *14*, 92.
[86] S. Jeong, H. Choi, J. Choi, C. Yu, J. O. Park, S. Park, *Sens. Actuators A* **2010**, *157*, 118.
[87] C. Yu, J. Kim, H. Choi, J. Choi, S. Jeong, K. Cha, J. O. Park, S. Park, *Sens. Actuators A* **2010**, *161*, 297.
[88] S. Floyd, C. Pawashe, M. Sitti, *IEEE Trans. Robot.* **2009**, *25*, 1332.
[89] I. S. M. Khalil, V. Magdanz, S. Sanchez, O. G. Schmidt, S. Misra, *IEEE Trans. Robot.* **2014**, *30*, 49.
[90] M. C. Hoang, K. T. Nguyen, V. H. Le, J. Kim, E. Choi, B. Kang, J. Park, C. Kim, *IEEE Trans. Syst. Man Cybern.* **2019**, *25*, 1332.
[91] H. Keller, A. Juloski, H. Kawano, M. Bechtold, A. Kimura, H. Takizawa, R. Kuth, in *IEEE RAS/EMBS Int. Conf. Biomedical Robotics and Biomechatronics*, IEEE, Rome **2012**, p. 859.
[92] D. Folio, A. Ferreira, *IEEE Trans. Robot.* **2017**, *33*, 583.
[93] K. B. Yesin, K. Vollmers, B. J. Nelson, *Int. J. Robot. Res.* **2006**, *25*, 527.
[94] L. Yang, Y. Zhang, Q. Wang, L. Zhang, *IEEE Trans. Biomed. Eng.* **2019**, *67*, 1517.
[95] H. Xie, X. Fan, M. Sun, Z. Lin, Q. He, L. Sun, *IEEE/ASME Trans. Mechatron.* **2019**, *24*, 902.
[96] I. S. M. Khalil, K. Youakim, A. Sánchez, S. Misra, in *IEEE/RSJ Int. Conf. Intelligent Robots and Systems*, IEEE, Chicago, IL **2014**, p. 4686.
[97] S. Scheggi, K. K. T. Chandrasekar, C. Yoon, B. Sawaryn, G. v. d. Steeg, D. H. Gracias, S. Misra, in *IEEE Int. Conf. Robotics and Automation*, IEEE, Singapore **2017**, p. 6156.
[98] J. Leclerc, B. Isichei, A. T. Becker, *IEEE Robot. Autom. Lett.* **2018**, *3*, 4367.
[99] J. Leclerc, H. Zhao, A. T. Becker, in *IEEE Int. Conf. Robotics and Automation*, IEEE, Montreal **2019**, p. 8890.
[100] C. Lee, H. Choi, G. Go, S. Jeong, S. Y. Ko, J. Park, S. Park, *IEEE/ASME Trans. Mechatron.* **2015**, *20*, 2067.
[101] U. W. Denzer, T. Rösch, B. Hoytat, M. Abdel-Hamid, X. Hebuterne, G. Vanbiervielt, J. Filippi, H. Ogata, N. Hosoe, K. Ohtsuka, *J. Clin. Gastroenterol.* **2015**, *49*, 101.
[102] A. Bigot, C. Tremblay, G. Soulez, S. Martel, *IEEE Trans. Robot.* **2014**, *30*, 719.
[103] O. Erin, M. Boyvat, M. E. Tiryaki, M. Phelan, M. Sitti, *Adv. Intell. Syst. 2020*, 2, 1900110.
[104] A. Becker, O. Felfoul, P. E. Dupont, in *IEEE/RSJ Int. Conf. Intelligent Robots and Systems*, IEEE, Chicago, IL **2014**, p. 2017.
[105] C. Dahmen, K. Belharet, D. Folio, A. Ferreira, S. Fatikow, *Int. J. Optomechatronics* **2016**, *10*, 73.
[106] B. E. Kratochvil, M. P. Kummer, S. Erni, R. Borer, D. R. Frutiger, S. Schürle, B. J. Nelson, *Experimental Robotic*, Springer, Berlin, Heidelberg **2014**.
[107] S. Salmanipour, E. Diller, in *IEEE Int. Conf. Robotics and Automation*, IEEE, Brisbane **2018**, p. 3608.
[108] D. Son, X. Dong, M. Sitti, *IEEE Trans. Robot.* **2019**, *35*, 343.
[109] I. S. M. Khalil, V. Magdanz, S. Sanchez, O. G. Schmidt, S. Misra, *Appl. Phys. Lett.* **2013**, *103*, 172404.
[110] E. Diller, M. Sitti, *Adv. Funct. Mater.* **2014**, *24*, 4397.
[111] J. Li, H. Wang, J. Cui, Q. Shi, Z. Zheng, T. Sun, Q. Huang, T. Fukuda, *Micromachines* **2019**, *10*, 370.
[112] À. Moya, M. J. Sancho-Tello, Á. Arenal, M. L. Fidalgo, R. Brugada, J. Martínez Ferrer, J. L. Merino, F. Ruíz Mateas, J. L. Mont, *Rev. Esp. Cardiol.* **2013**, *66*, 116.
[113] C. Chautems, A. Tonazzini, Q. Boehler, S. H. Jeong, D. Floreano, B. J. Nelson, *Adv. Intell. Syst.* **2019**, *2*, 1900086.
[114] A. Pourkand, J. J. Abbott, *IEEE Robot. Autom. Lett.* **2018**, *3*, 2957.
[115] E. S. Gang, B. L. Nguyen, Y. Shachar, L. Farkas, L. Farkas, B. Marx, D. Johnson, M. C. Fishbein, C. Gaudio, S. J. Kim, *Circ.: Arrhythmia Electrophysiol.* **2011**, *4*, 770.
[116] D. Filgueiras-Rama, A. Estrada, J. Shachar, S. Castrejón, D. Doiny, M. Ortega, E. Gang, J. L. Merino, *J. Vis. Exp.* **2013**, *74*, e3658.
[117] C. Chautems, B. J. Nelson, in *IEEE Int. Conf. Robotics and Automation*, IEEE, Shanghai **2017**, p. 4837.
[118] C. Chautems, A. Tonazzini, D. Floreano, B. J. Nelson, in *IEEE/RSJ Int. Conf. Intelligent Robots and Systems*, IEEE, Vancouver **2017**, p. 181.
[119] B. Véron, A. Hubert, J. Abadie, N. Andreff, in *IEEE/RSJ Int. Conf. Intelligent Robots and Systems*, IEEE, Tokyo **2013**, p. 4996.
[120] R. Chen, D. Folio, A. Ferreira, in *IEEE Int. Symp. on Medical Robotics*, IEEE, Atlanta, GA **2019**, p. 1.
[121] J. Sikorski, C. M. Heunis, F. Franco, S. Misra, *IEEE Trans. Magn.* **2019**, *55*, 1.
[122] L. Yang, X. Du, E. Yu, D. Jin, L. Zhang, in *IEEE Int. Conf. Robotics and Automation*, IEEE, Montreal **2019**, p. 9814.
[123] F. Ongaro, S. Pane, S. Scheggi, S. Misra, *IEEE Trans. Robot.* **2019**, *35*, 174.
[124] A. J. Petruska, J. B. Brink, J. J. Abbott, in *IEEE Int. Conf. Robotics and Automation*, IEEE, Seattle, WA **2015**, p. 149.
[125] C. M. Heunis, Y. P. Wotte, J. Sikorski, G. P. Furtado, S. Misra, *IEEE Robot. Autom. Lett. 2020*, 5, 704.
[126] G. Lucarini, M. Mura, G. Ciuti, R. Rizzo, A. Menciassi, *J. Med. Biol. Eng.* **2015**, *35*, 428.
[127] J. Edelmann, A. J. Petruska, B. J. Nelson, *Int. J. Robot. Res.* **2017**, *36*, 68.
[128] L. B. Kratchman, T. L. Bruns, J. J. Abbott, R. J. Webster, *IEEE Trans. Robot.* **2017**, *33*, 227.
[129] S. Jeon, A. K. Hoshiar, K. Kim, S. Lee, E. Kim, S. Lee, J. Y. Kim, B. J. Nelson, H. J. Cha, B. J. Yi, H. Choi, *Soft Robot.* **2018**, *6*, 54.
[130] F. P. Gosselin, V. Lalande, S. Martel, *Med. Phys.* **2011**, *38*, 4994.
[131] K. Zhang, A. J. Krafft, R. Umathum, F. Maier, W. Semmler, M. Bock, *Magn. Reson. Mat. Phys. Biol. Med.* **2010**, *23*, 153.
[132] A. D. Losey, P. Lillaney, A. J. Martin, D. L. Cooke, M. W. Wilson, B. R. H. Thorne, R. S. Sincic, R. L. Arenson, M. Saeed, S. W. Hetts, *Radiology* **2014**, *271*, 862.
[133] F. Settecase, M. S. Sussman, M. W. Wilson, S. Hetts, R. L. Arenson, V. Malba, A. F. Bernhardt, W. Kucharczyk, T. P. L. Roberts, *Med. Phys.* **2007**, *34*, 3135.
[134] A. J. Petruska, F. Ruetz, A. Hong, L. Regli, O. Sürücü, A. Zemmar, B. J. Nelson, in *IEEE Int. Conf. Robotics and Automation*, IEEE, Stockholm **2016**, p. 4392.
[135] J. Edelmann, A. J. Petruska, B. J. Nelson, *J. Med. Robot. Res.* **2017**, *03*, 1850002.
[136] M. Ilami, R. J. Ahmed, A. Petras, B. Beigzadeh, H. Marvi, *Sci. Rep. 2020*, 10, 2500.
[137] V. K. Venkiteswaran, J. Sikorski, S. Misra, *Mech. Mach. Theory* **2019**, *139*, 34.
[138] H.-L. Ching, M. F. Hale, M. E. McAlindon, *Ther. Adv. Gastroenter.* **2016**, *9*, 313.
[139] E. Morita, N. Ohtsuka, Y. Shindo, S. Nouda, T. Kuramoto, T. Inoue, M. Murano, E. Umegaki, K. Higuchi, *Gastrointest. Endosc.* **2010**, *72*, 836.
[140] S. Guo, Q. Yang, L. Bai, Y. Zhao, in *IEEE Int. Conf. Mechatronics and Automation*, IEEE, Changchun **2018**, p. 626.
[141] L. Arcese, M. Fruchard, A. Ferreira, *IEEE Trans. Robot.* **2013**, *29*, 1060.
[142] L. Zhang, J. J. Abbott, L. Dong, B. E. Kratochvil, D. Bell, B. J. Nelson, *Appl. Phys. Lett.* **2009**, *94*, 064107.
[143] S. Tottori, L. Zhang, F. Qiu, K. K. Krawczyk, A. Franco-Obregón, B. J. Nelson, *Adv. Mater.* **2012**, *24*, 811.

[144] G. Chatzipirpiridis, S. Gervasoni, C. Fischer, O. Ergeneman, E. Pellicer, B. J. Nelson, S. Pané, *Adv. Intell. Syst.* **2019**, *1*, 1900069.
[145] C. A. Koepele, M. Guix, C. Bi, G. Adam, D. J. Cappelleri, *Adv. Intell. Syst.* **2020**, 2, 2070052.
[146] R. Dreyfus, J. Baudry, M. L. Roper, M. Fermigier, H. A. Stone, J. Bibette, *Nature* **2005**, *437*, 862.
[147] T. Petit, L. Zhang, K. E. Peyer, B. E. Kratochvil, B. J. Nelson, *Nano Lett.* **2012**, *12*, 156.
[148] L. Zhang, T. Petit, Y. Lu, B. E. Kratochvil, K. E. Peyer, R. Pei, J. Lou, B. J. Nelson, *ACS Nano* **2010**, *4*, 6228.
[149] D. R. Frutiger, K. Vollmers, B. E. Kratochvil, B. J. Nelson, *Int. J. Robot. Res.* **2009**, *29*, 613.
[150] E. Diller, S. Floyd, C. Pawashe, M. Sitti, *IEEE Trans. Robot.* **2012**, *28*, 172.
[151] T. Xu, J. Zhang, M. Salehizadeh, O. Onaizah, E. Diller, *Sci. Robot.* **2019**, *4*, eaav4494.
[152] H. Lu, M. Zhang, Y. Yang, Q. Huang, T. Fukuda, Z. Wang, Y. Shen, *Nat. Commun.* **2018**, *9*, 3944.
[153] Z. Ren, W. Hu, X. Dong, M. Sitti, *Nat. Commun.* **2019**, *10*, 2703.
[154] W. Hu, G. Z. Lum, M. Mastrangeli, M. Sitti, *Nature* **2018**, *554*, 81.
[155] M. Boncheva, S. A. Andreev, L. Mahadevan, A. Winkleman, D. R. Reichman, M. G. Prentiss, S. Whitesides, G. M. Whitesides, *Proc. Natl. Acad. Sci. U. S. A.* **2005**, *102*, 3924.
[156] J. Kim, S. E. Chung, S. E. Choi, H. Lee, J. Kim, S. Kwon, *Nat. Mater.* **2011**, *10*, 747.
[157] Y. Kim, H. Yuk, R. Zhao, S. A. Chester, X. Zhao, *Nature* **2018**, *558*, 274.
[158] J. Yu, L. Yang, L. Zhang, *Int. J. Robot. Res.* **2018**, *37*, 912.
[159] J. Yu, B. Wang, X. Du, Q. Wang, L. Zhang, *Nat. Commun.* **2018**, *9*, 3260.
[160] H. Xie, M. Sun, X. Fan, Z. Lin, W. Chen, L. Wang, L. Dong, Q. He, *Sci. Robot.* **2019**, *4*, eaav8006.
[161] L. Yang, J. Yu, L. Zhang, *IEEE Trans. Robot. 2020*, 36, 254.
[162] Q. Wang, L. Yang, J. Yu, C. Vong, P. W. Y. Chiu, L. Zhang, in *IEEE/RSJ Int. Conf. Intelligent Robots and Systems*, IEEE, Madrid **2018**, p. 5380.
[163] J. Yu, D. Jin, K.-F. Chan, Q. Wang, K. Yuan, L. Zhang, *Nat. Commun.* **2019**, *10*, 5631.
[164] T. G. Leong, C. L. Randall, B. R. Benson, N. Bassik, G. M. Stern, D. H. Gracias, *Proc. Natl. Acad. Sci. U. S. A.* **2009**, *106*, 703.
[165] O. Ergeneman, G. Dogangil, M. P. Kummer, J. J. Abbott, M. K. Nazeeruddin, B. J. Nelson, *IEEE Sens. J.* **2008**, *8*, 29.
[166] Y. Zhang, L. Zhang, L. Yang, C. I. Vong, K. F. Chan, W. K. K. Wu, T. N. Y. Kwong, N. W. S. Lo, M. Ip, S. H. Wong, J. J. Y. Sung, P. W. Y. Chiu, L. Zhang, *Sci. Adv.* **2019**, *5*, eaau9650.
[167] X. Yan, Q. Zhou, J. Yu, T. Xu, Y. Deng, T. Tang, Q. Feng, L. Bian, Y. Zhang, A. Ferreira, L. Zhang, *Adv. Funct. Mater.* **2015**, *25*, 5333.
[168] F. Qiu, S. Fujita, R. Mhanna, L. Zhang, B. R. Simona, B. J. Nelson, *Adv. Funct. Mater.* **2015**, *25*, 1666.
[169] X. Yan, Q. Zhou, M. Vincent, Y. Deng, J. Yu, J. Xu, T. Xu, T. Tang, L. Bian, Y.-X. J. Wang, K. Kostarelos, L. Zhang, *Sci. Robot.* **2017**, *2*, eaaq1155.
[170] J. Park, C. Jin, S. Lee, J.-Y. Kim, H. Choi, *Adv. Healthc. Mater.* **2019**, *8*, 1900213.
[171] B. Wang, K. F. Chan, J. Yu, Q. Wang, L. Yang, P. W. Y. Chiu, L. Zhang, *Adv. Funct. Mater.* **2018**, *28*, 1870174.
[172] S. Kim, F. Qiu, S. Kim, A. Ghanbari, C. Moon, L. Zhang, B. J. Nelson, H. Choi, *Adv. Mater.* **2013**, *25*, 5863.
[173] Z. Lin, X. Fan, M. Sun, C. Gao, Q. He, H. Xie, *ACS Nano* **2018**, *12*, 2539.
[174] S. Tasoglu, E. Diller, S. Guven, M. Sitti, U. Demirci, *Nat. Commun.* **2014**, *5*, 3124.
[175] N. T. Nguyen, *Microfluid. Nanofluid.* **2012**, *12*, 1.
[176] E. Bormashenko, *Adv. Colloid Interface Sci.* **2019**, *269*, 1.
[177] T. Luo, L. Fan, R. Zhu, D. Sun, *Micromachines* **2019**, *10*, 104.
[178] H. D. Xi, H. Zheng, W. Guo, A. M. Gañán Calvo, Y. Ai, C. W. Tsao, J. Zhou, W. Li, Y. Huang, N. T. Nguyen, S. H. Tan, *Lab Chip* **2017**, *17*, 751.
[179] Y. Lvovsky, P. Jarvis, *IEEE Trans. Appl. Supercond.* **2005**, *15*, 1317.
[180] B. Wang, Y. Zhang, L. Zhang, *Quant. Imaging Med. Surg.* **2018**, *8*, 461.
[181] K. T. Nguyen, B. Kang, E. Choi, J. Park, C. Kim, *IEEE/ASME Trans. Mechatron.* **2020**, https://doi.org/10.1109/TMECH.2020.2974069.